Program and abstracts

In connection with the NIR (Network on Impact Research) workshop and excursion;

Gol, June 8. - 11., 2009

View towards Gol

Program for the Gardnos-Gol workshop and excursion

Monday 8. June:

1100: Departure from Gardermoen.

~1400: Arrival at Pers Hotel, Gol.

Lunch

Afternoon session
1500: Thomas Kenkmann:
"Structural geology of terrestrial impact craters"
Coffee break
1600: Andreas Jahn
"The deep structure of a collapsed central uplift - New insights into the development of the Vredefort Dome, South Africa"
1620: Sanna Holm
"The Siljan Impact Structure – A Short Review"
1640: Elin Kalleson
1 - "Introduction to the Gardnos impact crater"
2 - "Autochthonous impact breccias from the Gardnos structure - A study of deformation patterns"

2000: Dinner

Tuesday 9. June:

Breakfast

Morning session
0830: Axel Wittmann:
"Formation and Emplacement of Impatites in Large Terrestrial Impact Structures"
Coffee break
0930: Teemu Öhman
"Four hundred years of hits and misses in scientific impact crater research"
0950: Peter Somelar
"Structural state of smectite and mixed layer smectite-illite minerals as temperature indicator in impact induced hydrothermal systems: example of Ries crater"
1010: Nele Muttik
"Fluid temperature evolution in suevites at the Ries crater, Germany: stable isotope composition of smectite type minerals."
1030: Steven Goderis
"A geochemical characterization of the Gardnos impactor"

1050: Tom Jahren
“Update on geotourism projects in the Gardnos Meteorite Crater”

1200: Lunch

Excursion to Gardnos
- Introduction to the crater, get an overview of original and present shape, state of erosion, the general geological setting, visit localities of Gardnos Breccia.

2000: Dinner

Wednesday 10. June:

Breakfast

Morning session:
0830: Stephanie Christine Werner:
"The geophysical signature of impact craters"
0915: Kai Wünnemann:
"Scaling of crater formation - numerical modelling of impact processes on continental targets".
Coffee break
1015: Svein Olav Krøgli
“An impact crater detection tool (ICDY) applied to data from Finnmark, Norway”
1035: Ulla Preeden
“Preliminary paleomagnetic study of rocks from the possible impact structure at Åvikebukten Bay, Northern Sweden”
1055: Katerina Bartosova
“Chesapeake Bay impact structure - Investigations of the ICDP-USGS Eyreville drill core”

1200: Lunch

Excursion to Gardnos
- Visit localities of suevite and crater infill sediments

2000: Dinner

Thursday 11. June:

Breakfast

Morning session
0830: Galen Gisler:
"Calculations of asteroid impacts into deep and shallow water"
Coffee
0930: Thomas Kohout:
Scientific Opportunities for Human Exploration of the Moon’s Schrödinger basin

0950: Afsoon Moatari Kazerouni
“Petrography and diagenesis of Paleocene-Eocene sandstones in the Siri Canyon, Danish North Sea”
1010: Summary and discussion

1200: Lunch

1230: Departure

Arrival at Gardermoen ~1530.

Chesapeake Bay impact structure: Investigations of the impact breccia section (1397-1551 m) in the ICDP-USGS Eyreville drill core

Katerina Bartosova[1], Ludovic Ferrière[1], Dieter Mader[1], Christian Koeberl[1], and Uwe Reimold[2]. [1]Department of Lithospheric Research, University of Vienna, Althanstrasse 14, A-1090 Vienna, Austria (katerina.bartosova@univie.ac.at). [2]Museum für Naturkunde, Leibniz-Institute at Humboldt University Berlin, Invalidenstrasse 43, 10115 Berlin, Germany.

Introduction: The Chesapeake Bay impact structure (CBIS), 35 Myr old and 85 km in diameter, is the seventh largest impact structure currently known on Earth [1-3]. The CBIS is very well preserved, because it is situated on a passive continental margin and protected by overlying sediments [2]. Further, the CBIS is the source of the North American tektites [4].

The CBIS was drilled at Eyreville in 2005-2006 during an ICDP-USGS drilling project. Three drill cores (Eyreville A, B, and C), with a total depth of 1766 m, were recovered within the central zone of the structure, in the deep crater moat. The crater fill comprises post-impact sediments, sediment clast breccias and sedimentary megablocks (the so-called Exmore breccia beds), a large granitic and a small amphibolitic megablock, gravelly sand, impact breccia, and granites/pegmatites and mica schists (Fig. 1) [1]. About 150 samples from all the core depth, excluding the post-impact sediments were investigated. We have performed geochemical analyses and macro- and micro petrographic description of all the samples, but we have focused especially on the impact breccias [5] (the interval 1397-1551 m [6]).

Petrography of the impact breccias: The impact breccia section consists mostly of suevite and large blocks of gneiss. In the upper part (above ~1474 m) the suevite is melt-rich and contains two intervals (5.5 and 1 m thick) of impact melt rock [7]. In the deeper part of the impact breccia section (below 1474 m) melt-poor suevite and polymict lithic impact breccia alternate with large blocks of cataclastic gneiss. The suevite has a grayish, fine-grained clastic matrix and consists of a variety of rock and mineral clasts, melt particles, as well as secondary minerals. We have distinguished 6 different subunits of the impact breccia section (Fig. 1), based on the changes in the appearance of the suevite, e.g., abundance and types of lithic clasts and melt particles. The different types (subunits) of suevite suggest different modes of origin. The melt-poor bottom part with large clasts and blocks is probably of ground-surge origin. Towards the top, the proportion of fallback material increases; generally the abundance of melt particles increases and the clasts become smaller. The uppermost section with small clasts of all different types and shard-like melt particles represents fallback material.

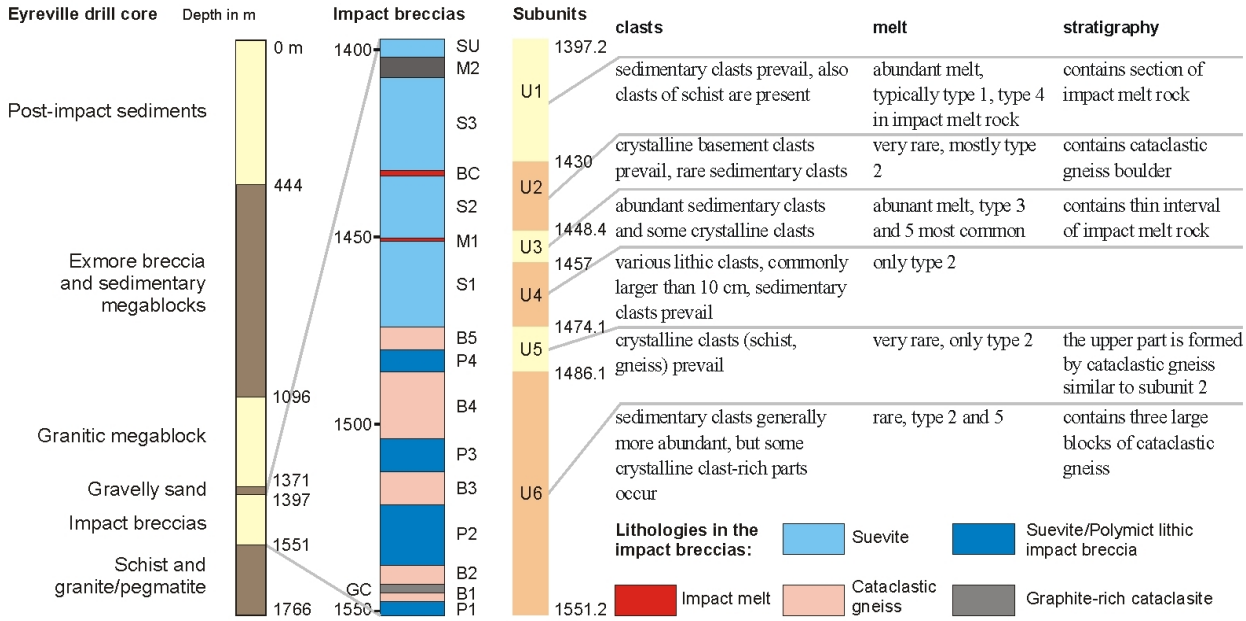

Fig. 1: Geologic column of the Eyreville drill core (left, after [1]), geologic column of the impact breccias (middle, after [6]), and subunits of the impact breccias (right).

Melt particles: Melt fragments are most abundant near the top of the impact breccia section (up to 34 vol% in the interval 1399-1422 m) and around 1450 m (up to 74 vol%). In the intervals 1402-1407.5 and 1450.2-1451.2 m, the suevite grades into impact melt rock. The millimeter- to centimeter-sized melt particles are mostly altered, commonly contain small undigested clasts (typically quartz) and show flow structures. Five major types of melt particles have been distinguished on the basis of color, micro-texture, and chemical composition: 1) clear, brownish, or greenish, unaltered glass, commonly with flow texture (dark and light colored schlieren) (Fig. 2); 2) brown melt, entirely altered to fine-grained phyllosilicate minerals, commonly with undigested clasts; 3) recrystallized silica melt; 4) melt with feldspar and/or pyroxene microlites; 5) dark brown melt (of shale precursor).

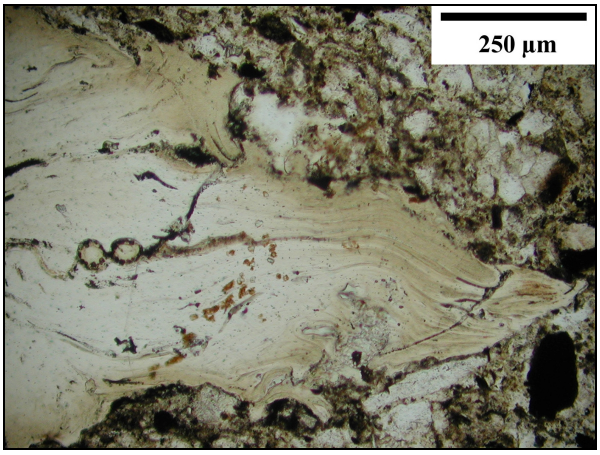

Fig. 2: Microphotograph (plane-polarized light) of a melt particle (type 1, clear to brownish/greenish unaltered glass), sample CB6-098, depth 1418.8 m, Eyreville B core.

Shock metamorphism: The shock and related features in the minerals of the impact breccia interval comprise abundant planar deformation features (PDFs; Fig. 3) and rare planar fractures (PFs) in quartz, rare PDFs in feldspar, and (not shock diagnostic) kink banding in mica. Toasted appearance of quartz is very common (Fig. 3) and ballen quartz was occasionally noted in the melt-rich samples.

Previous investigations of the proportions of shocked quartz grains (i.e., grains with PFs and/or PDFs) did not reveal any trends with depth [5], but noted that the average proportion of shocked quartz grains (sqg) in sedimentary clasts was higher compared to the crystalline clasts [5]. In an ongoing more detailed study of the shock effects in quartz we investigate relative proportions of sqg in clasts of different lithologies in suevite. The proportion of sqg in clasts is very variable, from 0 to more than 90 rel%. Generally, clasts with higher proportion of sqg become less abundant with increasing depth. Clasts with higher proportion of sqg were noted especially above ~1460 m. The clasts derived from the crystalline basement and sedimentary clasts with metamorphic overprint (i.e., the clasts from the deeper parts of the target) are generally less shocked (have mostly less than 10 rel% of sqg, although one granite clast with 58 rel% of sqg was noted). Clasts of polycrystalline quartz are relatively highly shocked (clasts with more than 20 rel% of sqg are common). The sedimentary clasts (i.e., the clasts from the upper part of the target) have a wide range of proportions of sqg (from 0 to >50 rel%) without any trends. This could be due to mixing of sedimentary clasts from different parts of the target area (sediments from the central part of the impact were more shocked than the sediments from the outer parts).

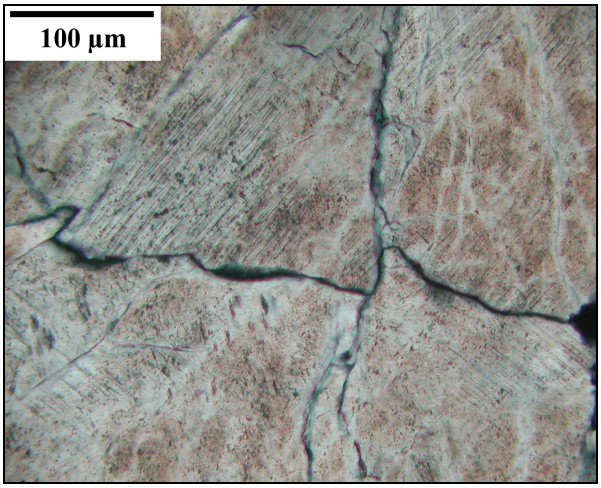

Fig. 3: Microphotograph (plane-polarized light) showing PDFs and toasted appearance of quartz in a granite clast in suevite. Sample CB6-100, depth 1427 m, Eyreville B core.

Acknowledgments: Drilling was supported by ICDP, USGS, and NASA, and executed by DOSECC. This work was supported by the Austrian Science Foundation (FWF), grant P18862-N10, to C.K.

References: [1] Gohn G. S. et al. (2006) *EOS* 87, 349 & 355. [2] Poag C. W. et al. (2004) The Chesapeake Bay crater: Geology and Geophysics of a late Eocene submarine impact structure, Impact Studies: Heidelberg, Springer, 522 p. [3] http://www.unb.ca/passc/ImpactDatabase/index.html [4] Deutsch A. and Koeberl C. (2006) *MAPS* 41: 689-703. [5] Bartosova K. et al. (2009) (Petrology) in: *GSA Special Paper (Chesapeake Bay Drilling Project volume)*, in press. [6] Horton J. W. et al. (2009) (Geologic column) in: *GSA Special Paper (Chesapeake Bay Drilling Project volume)*, in press. [7] Wittmann A. et al. (2009) (Melt rocks) in: *GSA Special Paper (Chesapeake Bay Drilling Project volume)*, in press.

CALCULATIONS OF ASTEROID IMPACTS INTO DEEP AND SHALLOW WATER

Galen Gisler, Physics of Geological Processes, University of Oslo

Contrary to received opinion, ocean impacts of asteroids do not produce tsunamis that lead to world-wide devastation. In fact the most dangerous features of ocean impacts are the atmospheric effects, just as for land impacts. I present illustrative hydrodynamic calculations of impacts into both deep and shallow seas, and draw conclusions from a parameter study in which the size of the impactor and the depth of the sea are varied independently. A brief summary of these follows.

Craters in the seafloor are produced when the water depth is less than about 5 times the asteroid diameter. Sediment removal and transport is important when the water depth is less than about 8 times the asteroid diameter. Both the depth and the diameter of the transient crater scale with the asteroid diameter, so the volume of water vapourised or excavated scales with the asteroid volume. The vapourised water (roughly a third of the crater volume) is of course unavailable to make a tsunami, though it may affect the climate later on. The rest of the crater volume goes into the splash and a propagating wave, roughly half and half. The wavelength is considerably shorter than for classical tsunamis, being only about twice the diameter of the transient crater. Even if propagation were perfect (which it most likely is not) the volume of water delivered per metre of shoreline is less than in the case of the Boxing Day 2004 tsunami for any impactor smaller than 500 metre diameter in an ocean of 5 km depth.

It is telling that the only "wet" crater for which tsunamis have definitely been proven is Chicxulub, which was in very shallow water. There of course the tsunami was most likely caused by slumps on the continental shelf made unstable by the violent shaking that the impact produced.

A GEOCHEMICAL CHARACTERIZATION OF THE GARDNOS IMPACTOR. S. Goderis[1], E. Kalleson[2], R. Tagle[1,3], H. Dypvik[4], R.-T. Schmitt[5], J. Erzinger[6], and Ph. Claeys[1], [1]Dept. of Geology, Vrije Universiteit Brussel, B 1050 Brussels, Belgium (Steven.Goderis@vub.ac.be), [2]Natural History Museum, University of Oslo, N-0316 Oslo, Norway, [3]Wisbyer Str. 35, D-13189 Berlin, Germany, [4]Dept. of Geosciences, University of Oslo, Norway, [5]Dept. of Mineralogy, Natural History Museum, Berlin, D-10099 Berlin, Germany, [6]GeoForschungsZentrum Potsdam, D-14473 Potsdam, Germany.

Introduction: The late Precambrian Gardnos impact structure (60°40′N, 9°00′E) is situated in Hallingdal, a valley about 125 km to the NW of Oslo, Norway. The deeply eroded structure comprises a circular area with a diameter of 5 km composed of impact-produced breccias and post-impact sedimentary rocks, emplaced within the Precambrian basement of South Norway.

During crater formation a small amount of meteoritic material (vapor and/or melt) can be incorporated into the impactites, resulting in a measurable geochemical signal in these molten and/or shocked rocks that difers from the crust-rock signature. This signal can confirm the impact origin of the structure and in some cases determine the precise nature of the projectile [1, 2]. For the Gardnos impact structure, previous studies had provided good evidence for the presence of a meteoritic component in the melt-matrix breccias based on the significantly enriched Ir and Os contents and the low $^{187}Os/^{188}Os$ ratios [3]. The goal of this study was to measure the concentrations of the platinum group elements (PGE) and Au, as well as the Ni and Cr content in the Gardnos impactites to characterize the type of impactor.

Methodologies: Fifteen impactite samples, predominantly impact breccias and suevites from the central and northeastern part of the Gardnos structure, were analyzed for platinum group elements (PGE) and Au using nickel-sulfide fire assay combined with inductively coupled plasma mass spectrometry (ICPMS). Major and trace elements were measured in the same samples using X-ray fluorescence (XRF). In addition, the concentrations of siderophile elements Ni, Cr, and Co were determined by ICP-MS after acid digestion.

Results: The samples show large variations in Ni (1–176 µg/g) and Cr (1–71 µg/g) contents. In the impactites, the Ni concentrations are significantly enriched compared to the average composition of the local continental crust. The distribution of the Ni and Cr concentrations seems non-uniform and may indicate that the cratering process added and/or redistributed these elements. The samples with the highest Ni concentrations are systematically found in the uppermost suevite layer associated with the highest Cr concentrations.

The measured PGE abundance in the Gardnos structure show a rather broad variation: for example Ir ranges from less than 0.040 ng/g to 1.926 ng/g. The samples collected at the contact between suevite and the sedimentary infill yielded the highest PGE concentrations (Ir=1.926 ng/g, Ru=3.494 ng/g, Pt=4.716 ng/g, Rh=0.766 ng/g, Pd=2.842 ng/g for GC6). This observation constitutes a persuasive argument for the presence of an extraterrestrial component in the Gardnos impactites. The 6 samples characterized by the most elevated Ni and Cr concentrations also yielded the highest PGE concentrations. The Ni and Cr concentrations show good correlation with each other and with Ir (R is > 0.96). The Ni/Cr ratio of the Gardnos impactor (2.56 ± 0.20) agrees with that of chondrites (2 to 7, [4]), whereas Ir is depleted relative to Ni and Cr in this projectile. The Gardnos impactites show a Ni/Ir ratio of 92,000 ± 8,000 compared to an average Ni/Ir ratio of 23,150 ± 4,250 for chondrites, while Gardnos has a Cr/Ir ratio of 35,000 ± 3000 compared to 690-10,470 in chondrites [4] (Fig. 1).

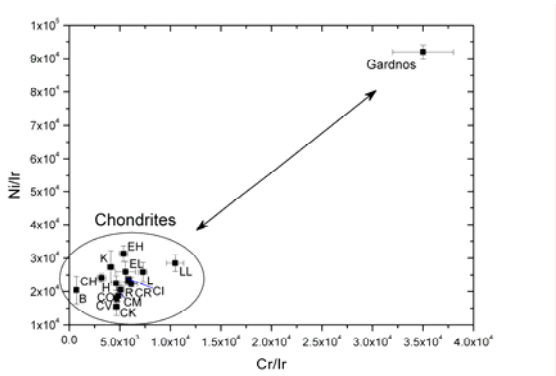

Fig. 1. Representation of a Ni/Ir versus Cr/Ir plot. The Gardnos impactor has a Ni/Ir and a Cr/Ir ratio that clearly differs from all chondites known today. The compiled data for chondrites are used from [4]. Uncommon abbreviation: B = Bencubbin; K = Kakangari.

The CI-normalized PGE patterns are characterized by Ru and Rh enrichments suggesting a nonchondritic impactor (Fig. 2). Concentration plots of the different PGE display an excellent correlation (R>0.99), indicative of a single source for the PGE enrichment. There is no clear indication of selective post-depositional remobilization of the characteristic highly siderophile elements. The averaged CI-normalized PGE concen-

trations of the Gardnos impactor exhibits similar inter-element ratios to the metallic phases of non-magmatic iron meteorites (NMI) (Fig. 2). Thus, the Ni/Ir and Cr/Ir data combined with the non-chondritic PGE ratios probably indicate a differentiated IA or IIIC non-magmatic iron meteoritic projectile.

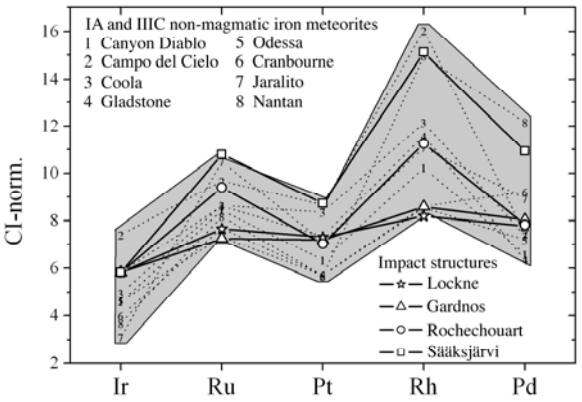

Fig. 2. Averaged CI-normalized PGE concentrations of the Gardnos impactor in comparison with those of the Rochechouart, Sääksjärvi, and Lockne impactors and the metallic phases of IA and IIIC NMI meteorites [5, 6]. The values of the impact structures have been multiplied with integer numbers (e.g., for Gardnos 4000) to allow a visual comparison of the element patterns.

Non-magmatic iron meteorites represent the second largest group of iron meteorites [7]. They underwent a complex and poorly understood formation history (e.g., metamorphism, partial melting, incomplete differentiation, crystal segregation, etc.; [8, 9]) that is reflected in the high variability of the amount of silicate inclusions [10]. After catastrophic impact breakup in the asteroid belt, gravitational reassembling of the debris produced a heterogeneous mixture of 5 different components: metal, sulfide-rich phase, chondritic-silicate phase, partial melt, and residues in almost random fractions. These components are mixed in different proportions in all known meteorites of this type [8].

Terrestrial impactor population: The projectile composition has been identified for approximately 40 of the 170 impact structures larger than 0.1 km recognized on Earth today, with varying degrees of accuracy mainly depending on the methodology used [e.g., 1]. So far iron meteorites only accounted for the formation of the majority of small impact craters, including for example the well-documented Barringer crater. The identification of the Gardnos projectile as one of four impact structures (together with Rochechouart, Sääksjärvi, and Lockne; Fig. 2) as a NMI, indicates that iron meteorites also form craters larger than just a few km. Based on the presently available data, the larger impact structures appear to be dominantly produced by the fall of chondritic projectiles, most commonly ordinary chondrites [1, 2]. The fossil meteorites recovered from the middle Ordovician limestones of Sweden are related to ordinary chondrites [11, 12]. A shower of OC projectiles is also advocated to explain the elevated bombardment rate in the late Eocene [13]. Non-magmatic irons now seem to represent the second most abundant group of projectiles recognized [14]. So far, the only carbonaceous chondrites recognized in the terrestrial stratigraphy are the 10 to 12 km in diameter Chicxulub projectile at the KT boundary, 65 million years ago [15, 16, 17] and the projectiles that created the Early Archean spherule beds S2, S3, and S4 of the Barberton greenstone belt in South Africa, between 3.2 and 3.5 Ga ago [18].

References: [1] Koeberl (2007) *In: Treat. of Geoch., online ed., Vol. 1, Elsevier*, 1.28.1 -1.28.52; [2] Tagle & Hecht (2006) *MAPS* 41, 1721-1735; [3] French et al. (1997) *GCA* 61, 873-904; [4] Tagle & Berlin (2008) *MAPS* 43, 541-559; [5] Tagle et al. (2009) *MAPS*, accepted for publication; [6] Tagle et al. (2008) *LPSC*, abstr. # 1418; [7] Grady (2000) *Cambridge Univ. Press*, 690 p.; [8] Benedix et al. (2000) *MAPS* 35, 1127-1141; [9] Wasson and Kallemeyn (2002) *GCA* 66, 2445-2473; [10] Mittlefehldt et al. (1998) *In: Planetary Materials. Mineral. Soc. of Am.*, 4.1–4.195; [11] Schmitz et al. (2001) *EPSL* 194, 1-15; [12] Greenwood et al. (2007) *EPSL* 262, 204-213; [13] Tagle and Claeys (2004) *Science* 305, 492-492; [14] Tagle et al. (2007) *LPSC*, abstr. # 2216; [15] Kyte (1998) *Nature* 396, 237-239; [16] Shukolyukov & Lugmair (2000) *Science* 282, 927-929; [17] Trinquier et al. (2006) *EPSL* 241, 780-788; [18] Kyte et al. (2003) *Geology* 31, 283-286.

THE SILJAN IMPACT STRUCTURE – A SHORT REVIEW. S. Holm[1], [1]Department of Geology, Geobiosphere Science Centre, Lund University, Sölvegatan 12, SE-22362 Lund, Sweden. E-mail address: Sanna.Holm@geol.lu.se.

The Siljan structure in south-central Sweden (61º2'N; 14º52'E) was first suggested to have been formed by the impact of a large extraterrestrial body based on observations of morphological features [1, 2]. Planar deformation features (PDF) in quartz [3, 4] and shatter cones [4] gave further support to the idea that the structure was in fact an impact crater. In a comparison with the Canadian impact structure Charlevoix, more information supporting an impactor origin also for Siljan was provided [5]. After the structure was confirmed as being impact derived there was a gap in research until the Deep Gas Drilling project was initiated in 1982 [6], as a consequence of the proposal that fractures below the crater could contain large amounts of trapped hydrocarbons derived from the mantle (The Deep-Earth-Gas hypothesis; [7]). After the closure of the project in 1991 (the gas found was not of any economic interest), Siljan seems to have been forgotten again, although many questions about the structure remain unanswered. For example, the diameter of the structure and the amount of erosion are not well constrained.

The Siljan structure is situated in the boundary zone between younger felsic intrusives belonging to the Trans-Scandinavian Igneous Belt (TIB) in the west, and older felsic extrusive and intrusive rocks to the east. Details on the regional geology of the Siljan area can be studied on a set of four bedrock maps covering the Siljan impact structure [11]. The central uplift, with a diameter of 32 kilometers, consists of felsic intrusives that belong to the TIB (Dala granites), with minor amounts of mafic representatives. Ordovician and Silurian sediments, although completely eroded in the surrounding area, have been preserved in a 10-kilometer wide ring-shaped depression surrounding the central uplift.

An apparent diameter of 52 kilometers is commonly given for the Siljan structure. This estimate was based on the present-day morphology of the structure [8], and coincides with the outer limit of the Paleozoic sedimentary ring. A larger diameter of 65 kilometers for the final crater was suggested based on structural geological considerations [9]. An even larger present-day diameter of 75 kilometers based on topographic features, and an original crater diameter of as much as 85 kilometers, based on the diameter of the crystalline core and seismic patterns seen in the central uplift, has also been suggested [10].

The structure has recently been given a new age of 377±2 Ma [12]. The material dated was interpreted to be impact melt breccia [12]. The occurrence of impact melt rocks associated with the structure needs to be further investigated, and to date, no definite identification of true impact melt rock has been made.

Although erosion of astroblemes on Earth provides unique information about the morphology and features of impact craters at depth, it complicates identifications of terrestrial impact structures, estimations of the original crater appearance and of conditions that prevailed at the time of impact. The Siljan impact structure is of Upper Devonian age [12], and thus great amounts of erosion have taken place until today, causing the central uplift of the structure to be eroded to the same level as the area surrounding Siljan. The erosion has actually been so extensive, that the surface presently exposed has been suggested to represent a level that was located below the original autochthonous crater floor [13]. Estimations about the pre-erosional appearance of Siljan are rare, and largely dependent on the amount of sediments that covered the crystalline basement at the impact location. However, descriptions about the sedimentary cover are contradictive. Traditionally, the sedimentary cover at the impact site has been described as 400-500 meters of Ordovician and Silurian sediments by e.g. [14]. At the present level of erosion, thermal indicators, e.g. $\delta^{18}O/\delta^{13}C$, conodont alteration indices (CAI), apatite fission tracks and lead mobility in basement rocks indicate raised temperatures of as much as 125ºC, a temperature increase attributed to burial by a much thicker sedimentary cover than 400-500 meters [15]. The thickness of these sediments, of Devonian age, in the central parts of Sweden has been estimated to have been ~2.5 kilometers at the approximate time of the impact that resulted in the Siljan structure [16, 17]. The sedimentary cover was composed of erosion products from the Caledonides, deposited in a Caledonian foreland basin [15, 16, 17]. These sediments have later been completely removed by erosion in Sweden.

A peak pressure of between 12-17 GPa indicated by the identification of planar deformation features in quartz grains [4, 18] retrieved from rock samples from the central parts of the structure, is about half as much as the expected peak pressure of 25-30 GPa that has been recorded in the rocks present at the central parts of terrestrial complex impact structures [13]. This in-

dicates that large amounts of rock constituting the original crater are missing.

The Deep Gas Drilling project resulted in large amounts of information about Siljan from seven shallow, and two deep, drillings. The most important scientific results of the drillings are summarized in [19], and much of the data have the potential to reveal much new information about the Siljan impact structure, if properly evaluated.

References: [1] Wickman F.E. et al. (1963) *Arkiv för Mineralogi och Geologi, 3,* 193-257. [2] Fredriksson K. and Wickman F.E. (1963) in Lundholm B. (ed.) *Svensk Naturvetenskap,* 121-157. [3] Svensson N.B. (1971) *Nature Phys. Sci., 229,* 90-92. [4] Svensson N.B. (1973) *GFF, 95,* 139-143. [5] Rondot J. (1975) *Bull. Geol. Inst. Univ. Uppsala, 6,* 85-92. [6] Bodén A. and Eriksson K. (eds.) *Deep Drilling in Crystalline Bedrock Vol. 1: The Deep Gas Drilling in the Siljan Impact Structure, Sweden and Astroblemes.* Springer Verlag, Berlin. 364 p. [7] Gold T. and Soter S. (1980) *Sci. Am., 242,* 130-137. [8] Grieve R.A.F (1982) *Geol. Soc. Am. Spec. Pap., 190,* 25-37. [9] Kenkmann T. and von Dalwigk I. (2000) *Meteoritics & Planet. Sci., 35,* 1189-1201. [10] Henkel H. and Aaro S. (2005) In Koeberl C. and Henkel H. (eds.) *Impact Tectonics*. Springer Verlag, Berlin, 247-283. [11] Kresten P. et al. (1991) Berggrundskartorna Ser. Ai, Nr 46, 48, 50 and 51. SGU. [12] Reimold W.U. et al. (2005) *Meteoritics & Planet. Sci., 40,* 591-607. [13] Grieve R.A.F. (1988) In Bodén A. and Eriksson K. (eds.) *Deep drilling in crystalline bedrock vol. 1: The deep gas drilling in the Siljan impact structure, Sweden and astroblemes.* Springer Verlag, Berlin, 328-348. [14] Rondot J. (1994) *Earth Sci. Rev., 35,* 331-365. [15] Tullborg E.L. et al. (1995) Thermal evidence of Caledonide foreland, molasse sedimentation in Fennoscandia. *Svensk Kärnbränslehantering AB technical report*, 38 p. [16] Larson S.Å. et al. (1999) *Terra Nova, 11,* 210-215. [17] Cederbom C. et al. (2000) *Tectonophysics, 316,* 153-167. [18] Åberg G. and Bollmark B. (1985) *Earth Planet. Sci. Lett., 74,* 347-349. [19] Juhlin C. (1991) *Scientific summary report of the Deep Gas Drilling Project in the Siljan ring structure*. Vattenfall U(G) 1991/14. 257 p.

THE DEEP STRUCTURE OF A COLLAPSED CENTRAL UPLIFT – NEW INSIGHTS IN THE DEVELOPMENT OF THE VREDEFORT DOME, SOUTH AFRICA.

A. Jahn[1], U. Riller[2] and W. U. Reimold[1]: [1]Museum für Naturkunde – Leibniz Institute at Humboldt University Berlin, Invalidenstrasse 43, D-10115 Berlin, Germany (Andreas.Jahn@mfn-berlin.de), [2]McMaster University, 1280 Main Street West, Hamilton, ON, L8S 4K1, Canada.

Introduction: In order to investigate the subsurface structure of the Vredefort dome (Fig.1), the central uplift of the 2.02 Ga Vredefort impact structure, structural, petrological and geophysical data [1, 2, 3] have been compiled, and numerical modeling [4] has been conducted. Based on these studies and new ground data, we constructed a 3D structural model for the upper parts of the central uplift. This model offers new insights into the structural inventory of tilted sedimentary rocks and the fault system of the collar. Our modeling results are consistent with an impact-induced suite of normal and reverse faults in this area and allows to link them to distinct stages of rock movements during the modification phase of cratering.

The Vredefort Dome is the eroded remnant of the collapsed central uplift structure [1]. The inner core of the Dome is approximately 40 km in diameter and consists mainly of Archean (> 3.1 Ga) granitoids and minor mafic intrusions. It is surrounded by the collar, an assembly of steeply dipping and overturned sedimentary and volcanic strata of Archean and Paleoproterozoic (3.07 - 2.1 Ga) age. To the north and west, the collar rocks are well exposed and form a series of concentric, morphologically prominent quartzite ridges, and intermittent valleys along less resistant shale horizons, wrapping around the crystalline core. To the east and in the south, the central uplift is largely covered by the Phanerozoic Karoo Supergroup and Quaternary deposits.

Methods: In field campaigns in 2007 and 2008 we collected structural data, mostly in the northern and western collar region, and created a detailed map of bedding plane orientations and faults identifiable in outcrop. In combination with seismic data and information from drill holes we constructed a 3D model of the respective collar strata with the software *ArcGIS* and *GOCAD*. For the visualization of the rock orientations we chose prominent lithological interfaces within the Archean sediments (West Rand and Central Rand Group) as marker surfaces. We also included a number of prominent dislocations known from previous field studies [6] and geophysical imaging. In order to test the plausibility of our results, we compared them to those predicted by numerical models [3].

The construction of a 3D multi-surface model characterized by impact-induced faults allowed us to identify coherent rock domains and their possible displacement during collapse of the central uplift. The model is limited by the exposure of pre-impact (meta)sedimentary rocks and, therefore, to the northern and western quadrants of the central uplift.

Results: The dips of inclined to steeply dipping, overturned sedimentary strata in the collar region increase from < 60° to 70-90° at a depth of 2 to 3 km. Hence, the current erosion surface is situated within the hinge zone between the steeply dipping strata and the overturned parts in the roof of the collapsed central uplift [4]. This observation of a transition zone agrees with erosion of 6 to 8 km. The dip of bedding planes also varies with the individual domains defined by faults. Generally, the bedding planes display maximum rotation in the northwest, but this may be blurred by differential rotation between adjacent domains.

On the km-scale, a significant number of faults is exposed in the collar. With respect to the center of the Vredefort Dome, most of them are either concentric [5] or radial faults [6]. Concentric faults strike parallel to the bedding in outcrop, but intersect the strata. Thus, thicknesses of strata are reduced by movements on concentric faults. Radial faults, however, are more curved at surface, listric in geometry, and displace concentric faults.

Conclusions: Our field structural analysis revealed the existence of a set of faults with variable orientations and truncation relationships. The observed fault geometry supports the hypothesis of a complex impact-related fault system comprising normal and reverse faults in a close genetic context.

The geometry and geometric relationship of bedding and fault surfaces point to impact-induced deformation. The shape and post-impact orientation of the faults with respect to orientation of bedding planes excludes an origin of the faults in their current orientation. Concentric faults formed likely by reverse slip toward the crater center and appear to be younger than the collapse of the central uplift. By contrast, concentric faults are displaced by radial ones, which were tilted later. Consequently, the concentric faults must have formed during an early stage of crater modification.

Back rotation of the collar strata to their pre-impact orientation leads us to the following kinematic model of faulting during central uplift formation.

Back rotation of the concentric faults by the same rotation magnitude as bedding planes suggests an

origin of these faults as normal faults. Thus, concentric faults are likely relics of discontinuities accomplishing terracing of the rim of the transient cavity (Fig. 2a). The geometry of concentric faults was subsequently modified by radial faults which formed as reverse or thrust faults. Overall, the fault kinematics point to a constrictional rock flow, which is compatible with the formation of the central uplift by crater-inward mass flow (Fig. 2b, c). As a consequence of convergent rock flow toward the crater center, the strata and faults were uplifted and rotated as well as displaced outwards with respect to the crater center (Fig 2d).

References: [1] Reimold W.U. and Gibson R.L. (2006) *Chemie der Erde, 66,* 1–35. [2] Lana C. and Gibson R. L. (2006) *S. Afr. J. of Geol., 109,* 265-278. [3] Henkel H. and Reimold W.U. (2002) *J. of Applied Geophys.,* 43–62. [4] Ivanov B. (2005) *Solar System Research, 39,* 381-409. [5] Grieve R.A.F., Reimold W.U., Morgan J., Riller U. and Pilkington M. (2008) *Meteorit. Planet. Sci*., 43, 855-882. [6] Bisshoff A.A. and Mayer J.J. (1999), *Council for Geoscience, Pretoria*, Geol. Map 1:50.000.

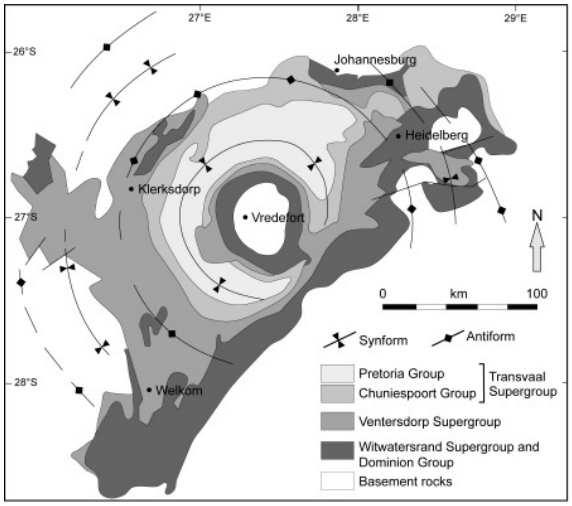

Figure 1: Map of the Witwatersrand Basin. The centrally located Vredefort Dome with its uplifted basement rocks and metasediments is structurally limited by the Potchefstroom Synclinorium.

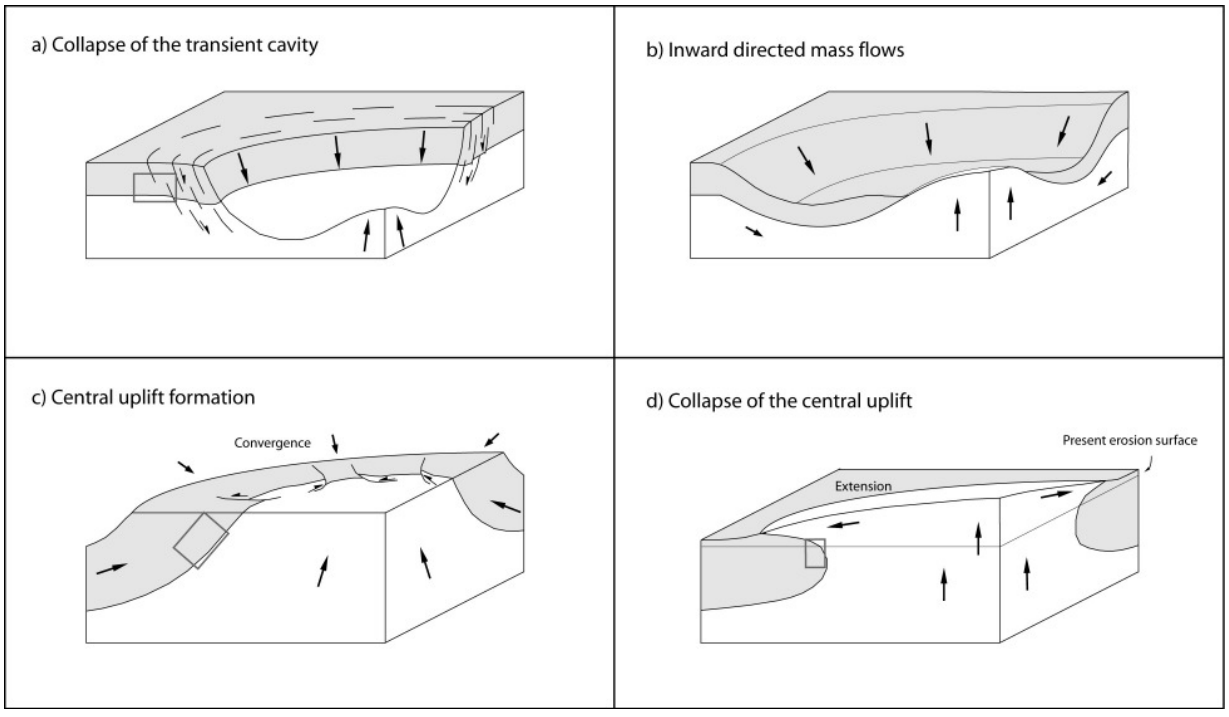

Figure 2: Summary of succession of mass movements during the modification stage of the Vredefort impact. Arrows indicate movement directions of rocks, boxes represent the current level of exposure.
(a) Early modification phase: the rim of the transient cavity collapses. Besides listric terraces of the crater walls smaller listric normal faults develop in concentric orientation. (b) At the collapse of the crater rim inward-directed mass flow contributes to the growth of the central uplift. (c) Convergent mass movements form an uplift in the center of the structure. Compression leads to the formation of reverse faults that become gradually rotated upwards. (d) The uplift growth reaches its vertical limit and the central peak begins to collapse outward, with the upper strata undergoing strong rotation.

AUTOCHTHONOUS IMPACT BRECCIAS FROM THE GARDNOS STRUCTURE – A STUDY OF DEFORMATION PATTERNS. E. Kalleson[1], H. Dypvik[2], T. Jahren[3], [1]Natural History Museum, University of Oslo, 0316 Oslo, Norway, (elinkal@geo.uio.no), [2]Dept. of Geosciences, University of Oslo, 0318 Oslo, Norway, [3]Rambøll.

Introduction: The most famous impactite from the Gardnos impact structure is the so-called Gardnos Breccia, first described by Broch [1]. Apart from being subject to scientific studies [2, 3], it has been utilized for different commercial purposes ranging from material for road construction to local art and jewelry. Typically the Gardnos Breccia appears with cm- to dm-sized white/light grey quartzitic/granitic fragments in dark grey to black matrix. However, mapping this breccia in field reveals large local variations in the relative amounts of matrix and larger lithic fragments. During impact these lithologies were exposed to violent pressure waves penetrating deep into the ground, and constitute the former crater floor. This study presents results from field observations and systematical mapping, illustrating the variations in appearance of the breccias, but also indicating some general connections between local target lithologies, distance from crater centre and the brecciation patterns.

Results: The target area of the Gardnos impact crater is often described as "mainly crystalline basement", but at a closer look it is a variety of different lithologies. Precambrian granites, granitic gneisses, quartzite and some banded gneisses dominate in the area, appearing in zones striking approximately north-south. In addition some darker, amphibolitic rocks (described as meta-gabbros and meta-dolerites at the regional geological map by NGU [4]) occurs as rock bodies of limited extent several places within the crater structure.

The granite/granitic gneiss and most of the quartzites behaved in a brittle manner; fracturing into relatively small pieces (generally < 10 cm) during impact. The breccia consists of light coloured rock fragments in a dark matrix of finely crushed rock material (also containing a little carbon) and makes up the typical "Gardnos Breccia". However, thin section observations indicate that very little or no deformation occurs within the rock clasts. Banded gneiss occurs only at a few localities, where it is generally fractured into larger (10-30 cm) clasts. Because of the characteristic banding patterns it offers a rare opportunity to study the displacement and rotation of clasts due to the movements of the ground during impact. A black quartzite is found within the area generally covered by Gardnos Breccia. At field and hand specimen scale the quartzite appears to be unbrecciated. Also the amphibolitic rocks generally seem to have avoided brecciation. Being resistant to erosion the amphibolitic rocks often stand as topographic highs, and they make up a large part of the central uplift. Though the black quartzite and the amphibolitic rocks do not brecciate in the typical large-scale "Gardnos Breccia patterns" they may show breccia patterns on a microscopic scale. The black quartzite is penetrated by numerous thin fractures, some lined with carbon. This is probably the explanation of the black colour. The amphibolitic rocks in general seem to be unaffected by the impact. Only in the samples taken at the central uplift brecciation at microscopic scale is common.

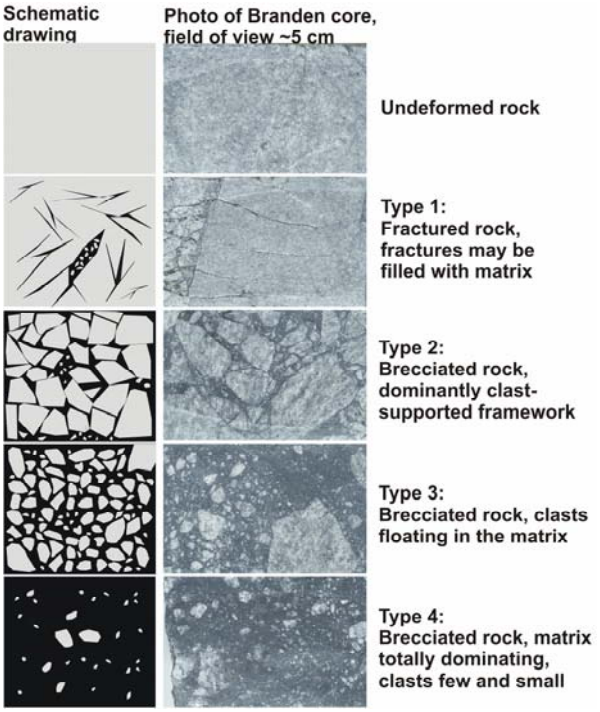

Fig. 1. Brecciation patterns observed in Gardnos Breccia rocks ranging from fracturing to almost complete disintergration into matrix-dominated rocks with only few larger rock fragments preserved.

Conclusions: This preliminary study indicates that in the granitic and quartzitic rocks most of the deformation resulted in matrix generation, whereas in the amphibolitic rocks no matrix was generated though deformation in some cases took place at a microscopic scale. The degree of brecciation varies considerably also within each lithology type, even over short distances (few meters to tens of meters). On large scale, however, there is a general trend towards less brecciation with increasing radial distance to the crater centre.

References: [1] Broch (1945) *Norsk geologisk tidsskrift 36, 16-25*; [2] French et al. (1997*), Geochimica et Cosmochimica Acta 61, 873-904;* [3] Gilmour et al. (2003), *Geochimica et Cosmochimica Acta 67, 3889-3903;* [4] Nordgulen et al. (1997) *Geological map M 1: 100 000 of Nes county, Norway: Geological Survey of Norway.*

Petrography and diagenesis of Paleocene-Eocene sandstones in the Siri Canyon, Danish North Sea

[1]A. M. Kazerouni , [2] H. Friis , [3] Johan B Svendsen,
[1 & 2] Geologisk Institut -Aarhus University (Denmark), [3]DONG Energy (Denmark)

Introduction: Post-depositional remobilization and injection of sand are often seen in deepwater clastic systems and has been recently recognised as a significant modifier of deep-water sandstone geometry.

Large-scale injection complexes have been interpreted in the Paleocene Siri Canyon near the Danish Central Graben of the North Sea hydrocarbon province from borehole data (Fig.1).

The emplacement of largescale injection complexes has been commonly recognized in the geological literature to seismic activity and consequent sand liquefaction.

However, as a result of very small differences in textural and compositional properties, and the lack of depositional structures often seen in deep-water sand, the distinction between "in situ" and injected or remobilised sands is indistinct.

Large scale heavy mineral sorting (in 10 m thick units) is observed in several reservoir units and has been interpreted to signify the depositional sorting.

Heavy mineral sorting does also occur in injected sands and a detailed understanding of this sorting process is essential when evaluating the origin of a sediment.

In his study we demonstrate an example of effective sorting of heavy minerals in a thin injected sand where the sorting is related to the flow patterns during injection.

Differences in sorting pattern of heavy minerals are suggested as a tool for petrographic /geochemical distinction between "in situ" sands and their related injected sands, particularly where potential primary structures are removed.

Studied glaconitic sandstones reservoir in the Siri Canyon are based on the investigatation of the geochemical composition of the reservoir sand in cores and also petrographic investigations by optical microscope, scanning electron microscope (SEM) examinations and XRF analyses .

Depositional and remobilized sandstone units are identified in cores from the Paleocene sand-rich Cecilie-wells which provides this study with examples of heavy mineral sorting in depositional and remoblised sandstones.

The deposition and sorting of heavy mineral grains in these sediments is controlled mainly by grain size, shape and density (Fig.2).

Heavy minerals may be selectively concentrated during transport and deposition because of their high density.

Selective concentration of heavy minerals is thought to take place through a combination of sorting mechanisms, including settling velocity and differential transport and entrainment.

This study also presents the occurrence and compositional variation of the authigenic zeolites in the Siri Canyon sandstones, and discuss the physicochemical conditions which prevailed during formation of zeolites, pore water chemistry, composition of mineralogical precursors and the host sediments.

Studied zeolites in Siri Canyon have a hydrated alumosilicate framework with varying amounts of alkali and alkaline earth metals.

Authigenic zeolites may be common in deep marine sediments, and in volcanoclastic deposits.

They are generally related to dissolution of siliceous fossils or diagenetic alteration of volcanic glass (Fig.3).

Authigenic zeolites are uncommon constituents in most sandstone.

However, authigenic zeolites are common in some of the glauconitic sandstones from the Siri Canyon, where it is generally associated with thick coatings of opal/microquartz on the detrital framework grains.

References:

[1]Hamberg, L., Dam, G., Wilhelmson, C. & Ottesen, T.G. (2005): Paleocene deep-marine sandstone plays in the Siri Canyon, offshore Denmark – southern Norway. In: Doré, A.G. & Vining, B.A. (eds): Petroleum geology: North-West Europe and global perspectives. Proceedings of the 6th petroleum geology conference, 1185–1198. London: Geological Society.

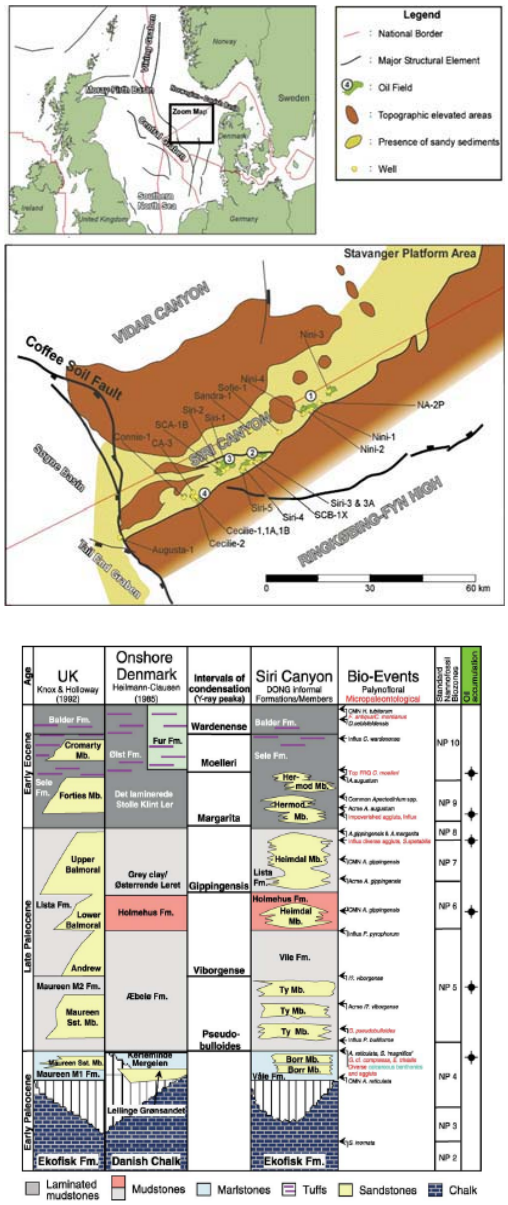

Fig.1.Paleocene-Lower Eocene Location map and schematic stratigraphy infill of the DanisNorth Sea and Siri Canyon. Taken from Hamberg, L. et al. (2005) [1]

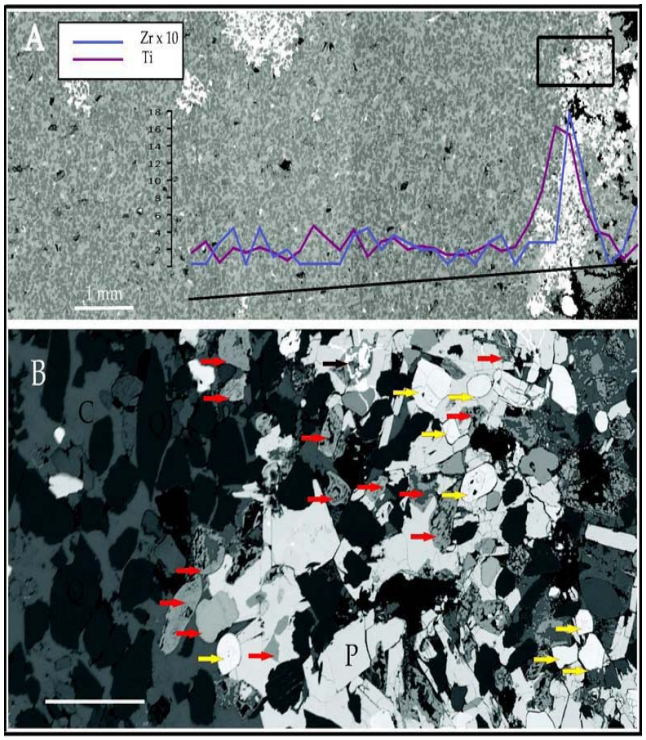

Fig.2. A Combined SEM-BSE micrograph of thin section (CE-2 2316.15m). EDAX-data along black line. Scale is 18W% for Ti, 1,8W% for Zr. White areas are cemented by pyrite. Black box indicates close up in B. B) SEM-BSE micrograph of HM laminas. Red arrows indicate Ti-rich mineral grains, yellow arrows indicate zircon grains. Q : quartz grain; C: calcite cement, P : pyrite; black arrow point to barite in fracture. Note that quartz grains in HM lamina are significantly smaller than quartz grains in host sediment.

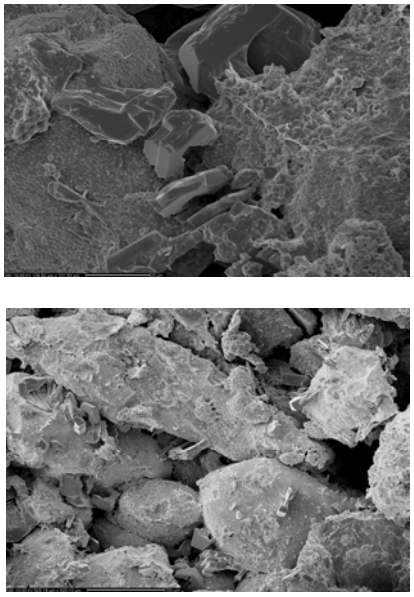

Fig.3. Predictive model of zeolite-mineralization is potentially applicable to other sandstone reservoirs with a volcanic ash component. Overall, recovery can be increased by recognizing specific zeolites and properly treating the wells with appropriate completion fluids to minimize formation damage and the resulting production loss.

SCIENTIFIC OPPORTUNITIES FOR HUMAN EXPLORATION OF THE MOON'S SCHRÖDINGER BASIN. T. Kohout[1, 2, 3], K. O'Sullivan[4], A, Losiak[5], K. G. Thaisen[6], S. Weider[7, 8] and D. A. Kring[9], [1]Department of Physics, University of Helsinki, Finland, tomas.kohout@helsinki.fi, [2]Department of Applied Geophysics, Charles University in Prague, Czech Republic, [3]Institute of Geology, Academy of Sciences of the Czech Republic, Prague, Czech Republic, [4]Department of Civil Engineering and Geological Sciences, University of Notre Dame, Notre Dame, IN, USA kosulli4@nd.edu, [5]Michigan State University, East Lansing, MI, USA, [6]University of Tennessee, Knoxville, TN, USA, [7]The Joint UCL/Birkbeck Research School of Earth Sciences, London, UK, [8]The Rutherford Appleton Laboratory, Chilton, Oxfordshire, UK, [9]Lunar and Planetary institute, Houston, TX, USA.

Introduction: The Schrödinger impact basin provides a rich array of scientific opportunities due to its location in a previously unexplored region of the Moon and a relatively young age. Located near the South Pole on the lunar far side, it is the second youngest impact basin (after Orientale) and, thus, remains well exposed for scientific study. Schrödinger intersects the pre-Nectarian Amundsen-Gainswindt basin (AG), as well as the inner rings of the South Pole-Aitken (SPA) basin. Modeling suggests [1] that Schrödinger's inner ring originates from a depth of 10-30 km and, therefore, might contain indigenous SPA materials. Additionally, at least three volcanic units, deep fractures, ghost craters, and secondary craters can be found within Schrödinger basin.

Main scientific objectives for human exploration within Schrödinger basin: The following major scientific goals can be accomplished within Schrödinger [2], which address many National Research Council lunar science priorities [3]:

1. Determine the age of the Schrödinger impact event.
2. Determine the age of material from Schrödinger's inner ring. In the case that SPA material is uplifted there, the SPA event can be dated allowing us to anchor the Earth-Moon impact flux curve.
3. Study material produced by various basaltic volcanic events (Upper Imbrian and Eratosthenian in age [4, 5]).
4. Study deep seated explosive volcanism (Eratosthenian or Copernican in age [4, 5]).
5. Study potential products of crustal and mantle degassing along deep fractures.
6. Study ghost craters flooded by a melt sheet.
7. Study secondary craters on the basin floor.

Landing site selection: We propose a landing site for human exploration on a relatively smooth terrain ([4, 5]) within the inner ring of Schrödinger – either on the exposed melt sheet or on one of the basaltic units. Such a location will provide access to the features outlined above and meet a planned ~20 km extra vehicular activity (EVA) limit [2]. Based on geological mapping [4] and Clementine images, we evaluated three landing sites (Fig. 1) where at least 4 of the scientific objectives can be accomplished. The white circles in Fig. 1 outline a 10 km radius of an EVA range (~20 km return trip).

The first landing site is located on the northern part of the Schrödinger melt sheet where a basaltic unit is superimposed. This relatively smooth terrain should ensure safe landing conditions. The basaltic unit might be the first sample station. It is approx. 5 km across in its shorter dimension and, thus, can be completely traversed before proceeding farther south to one of two facies of Schrödinger's melt sheet, providing a second point of interest within a single EVA. A second EVA to the southwest provides access to a second basaltic unit. A third EVA towards the west of the landing site will take crew to the second of the two melt facies and to one of the deep fractures on the basin floor. From those stations, crew can move north to Schrödinger's inner ring. Additionally, an Orientale secondary crater is located east of one of the basaltic units in a rougher terrain that could be targeted by additional EVA's .

A second landing site is located in the western part of the Schrödinger's melt sheet, near two large ghost craters that appear to have been flooded by the melt sheet during the complex formation of the basin. This provides the first opportunity for crew to study the morphology of a ghost crater and the thickness of a basin melt sheet. Towards the east, a ridged terrain of unknown origin as well as Antoniadi secondary craters can be reached. Towards the west, Schrödinger's inner ring is accessible for additional sampling of potential SPA material.

A third landing site is proposed in the southeastern part of the basin to study an explosive volcanic unit. The central volcanic crater, as well as crustal fractures through which magma may have migrated towards the surface, occur within EVA limits. Additionally, Schrödinger's inner ring is accessible to the southeast and Antoniadi secondary craters occur towards the west. One of the impact melt facies is located near the landing site and, if routes across basin fractures can be found, the other facies can also be reached. This option, however, must be evaluated with additional work.

The use high-resolution imagery, spectroscopic data, and digital elevation models can be used within a

Geographic information system (GIS) to identify locations of high interest for EVA. In addition, a GIS can be used to assess potential EVA routes and to maximize hazard avoidance by characterizing surface parameters (i.e., slope angle, slope aspect, roughness, composition, etc.) prior to surface operations [6].

Additionally, a precursor robotic rover can reduce the risk, requirements, and cost of a human exploration [7, 8] and provide site characterization to enhance the efficiency of human exploration by identifying the highest priority traverse stations. It could also collect and deliver samples from remote areas to the human mission landing site or conduct complementary research after the human mission departure [7, 8].

Conclusions: The Schrödinger basin provides a diverse suite of scientific opportunities because of the superposition of several geologic processes and because of its relatively young age. Any one of three possible landing sites can provide the first samples of basin melts of undisputable origin and potentially melts of SPA origin. In addition, at least two types of younger volcanism (and magmatic source regions) can be studied in the area with a small number of EVA's.

Acknowledgements: This work is part of the 2008 Lunar Exploration Summer Intern Program at the LPI, Houston, and co-sponsored by the NASA Lunar Science Institute. We thank the LPI staff for their help and support.

References: [1] Cintala M. J. and Grieve R. A. (1998) *MAPS, 33*, 889-912. [2] O'Sullivan K. et al. (2008) *Joint Annual Meeting of LEAG-ICEUM-SRR*, Abstract #4081. [3] National Research Council, *The Scientific Context for Exploration of the Moon* (2007). [4] Shoemaker E. M. et al. (1994) *Science, 266,* 1851–1854. [5] Mest S. C. and Van Arsdall L. E. (2008) *NSLI Lunar Science Conference,* Abstract #2089. [6] Thaisen K. G. et al. (2008) *Joint Annual Meeting of LEAG-ICEUM-SRR*, Abstract #4098. [7] Kohout et al. (2007) *Joint Annual Meeting of LEAG-ICEUM-SRR*, Abstract #4078. [8] Kring D. A. (2007) *LEAG Workshop on Enabling Exploration*, Abstract #3037.

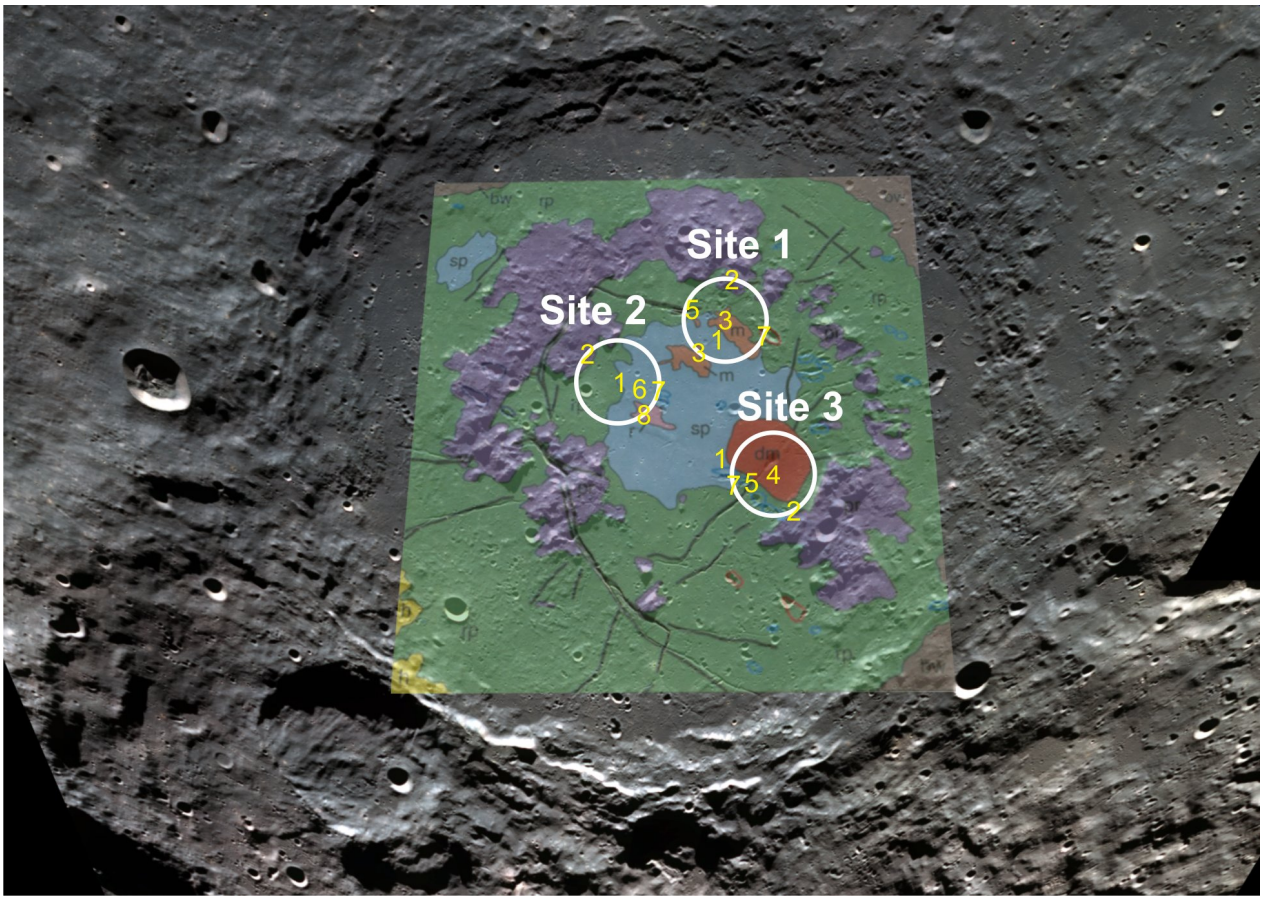

Figure 1: The Clementine image of the Schrödinger basin with the geological map from [4]. The three landing sites and corresponding 10 km EVA radius (20 km return trip) are outlined in white. The yellow numbers correspond to following scientific points of interest: 1 – Schrödinger's melt sheet, 2 – Schrödinger's inner ring, 3 – basaltic units, 4 – explosive volcanic unit, 5 – deep crustal fractures, 6 – ghost craters, 7 – secondary craters, 8 – ridged terrain.

AN IMPACT CRATER DETECTION TOOL (ICDY) APPLIED TO DATA FROM FINNMARK, NORWAY. S. O. Krøgli[1], H. Dypvik[1], A. Chicarro[2], L. J. Pesonen[3], A. P. Rossi[4] and B. Etzelmüller[1], [1]Department of Geosciences, University of Oslo, P.O.Box 1047, NO-0316 Oslo, Norway, (sveinkro@geo.uio.no), [2]ESA/ESTEC, Solar System Missions Division, Postbus 299, 2200 AG Noordwijk, The Netherlands, [3]Division of Geophysics, University of Helsinki, P.O. Box 64, FI-00014 Helsinki, Finland, [4]International Space Science Institute (ISSI), Hallerstrasse 6, CH-3012 Bern, Switzerland.

Introduction: A crater detection and recognition tool developed by the European Space Agency (ESA) and LogicaCMG UK [1] has been applied to digital elevation models (DEM), Landsat multispectral images and lake data from Finnmark, northern Norway. The impact crater discovery (ICDY) tool was designed to explore multi-mission terrestrial data (optical and multispectral images, SAR and DEM), where unknown impact structures might be discovered.

Fresh impact craters are characterized by their often circular shape [e.g. 2]. On Earth active geological processes will, however, eventually modify this surface expression. Still, the diverse terrestrial impact structure catalogue suggests the use of a simple detection characteristic, the circular shape. The ICDY tool makes use of the radial consistency algorithm that calculates the amount of circular symmetry about a point [3].

Circular symmetry: The radial consistency algorithm is a moving window operation evaluating differences in pixel values along and between profiles (default 16 profiles) radiating from a centre pixel [3]. An area of circular symmetry have altogether larger pixel contrast differences along radial profiles than between adjacent profiles. A value *(A-B)-(A-C)* is calculated, where the considered pixel is named *A*, the next pixel outward in the profile is named *B* and the pixel on profile to the right, but on the same level as *A* is named *C* (Fig. 1). This value is summarized for all pixels on profiles in the window, before the window moves to next step. At each step the value is modified to make the calculation more dependent upon geometry than contrast differences, e.g. black or grey circles on a white background would get similar values. The result is a crater likelihood image (CLI). High values indicate that the pixel is the centre of a region of circular symmetry. These pixels are later isolated by a peak detection technique or a simple CLI threshold. The most probable radius of each site is the radius that contributes most to the CLI value. Results from multiple data sources should be comparable due to the modifying step.

Results and discussion: A crater counting exercise comparing automatic and manually detected craters on Mars showed that a CLI threshold of 2.2 seem reasonable for a broad range of topographies and data, being a compromise between detecting too many false positives or leaving too many craters undetected. While impact craters often appear distinct on planetary bodies, the objective with such a method on Earth would usually be to detect one or a few candidates before conducting field observations and laboratory analyses to determine their origin. Fig. 2 displays detected features. There were no significant feature overlaps between the different data. A stricter CLI threshold and a morphology filter may refine the number of candidates found using the DEM. A less strict CLI threshold should be used for Landsat data. In this data there was a tendency of water being attractive to the algorithm, favoring circular lakes, due to the large contrast between water and other surfaces. The algorithm approach makes it applicable to include e.g. airborne geophysical data, which cover most of the Nordic countries, in future studies.

References: [1] Earl J. et al. (2005) *LPSC XXXVI*, abstract #1319. [2] Melosh H. J. (1989) *Impact cratering, a geologic process*. [3] Bruzzone L. et al. (2004) *In Proc. ESA-EUSC*, 13.1.

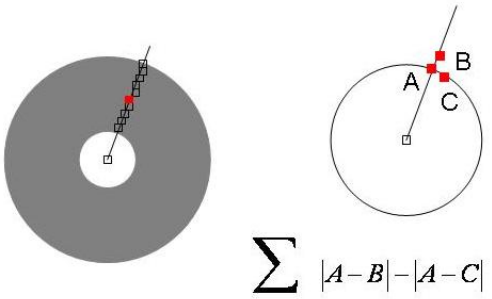

Fig. 1: Radial consistency setup. Grey area on left circle is the search radius for centre pixel. One of the sixteen radii/profiles is displayed with pixels. For each pixel on profile the value *(A-B)-(A-C)* is calculated, where the pixel *C* is on a radii/profile to the right of the considered one. This is summarized for all pixels on all the sixteen radii/profiles.

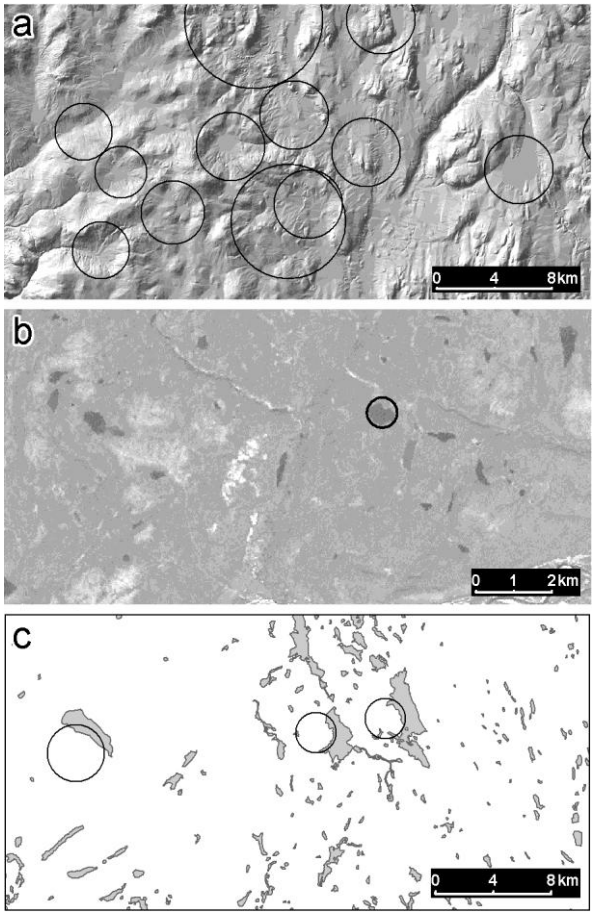

Fig. 2: Automatic detected regions of circular symmetry in three different regions using three different data sources. The figures are from Finnmark county, an area dominated by Precambrian basement rocks. CLI > 2.2 in all images. Search diameters comprised between 1 and 40 km for (a) a DEM of 100 m spatial resolution, (b) a Landsat image of 30 m spatial resolution and (c) a map of lakes (converted to raster data of 25 m spatial resolution before analysis).

FLUID TEMPERATURE EVOLUTION IN SUEVITES AT THE RIES CRATER, GERMANY: STABLE ISOTOPE COMPOSITION OF SMECTITE TYPE MINERALS. N. Muttik[1], K. Kirsimäe[2], G. R. Osinski[3], P. Somelar[4] and T. W. Vennemann[5], [1]Department of Geology, University of Tartu, Vanemuise 46, 51014 Tartu, Estonia, nele.muttik@ut.ee, [2]Department of Geology, University of Tartu, Vanemuise 46, 51014 Tartu, Estonia, kalle.kirsimae@ut.ee, [3]Departments of Earth Sciences/Physics and Astronomy, University of Western Ontario, 1151 Richmond Street, London, ON, N6A 5B7, Canada, gosinski@uwo.ca, [4]Department of Geology, University of Tartu, Vanemuise 46, 51014 Tartu, Estonia, peeter.somelar@ut.ee,.[5]Institute of Mineralogy and Geochemistry, University of Lausanne, Building Anthropole, CH-1015 Lausanne, Switzerland, torsten.vennemann@unil.ch.

Introduction: The 24-km diameter Ries impact crater, southern Germany exhibits well-preserved crater fill and surficial suevite deposits that are altered to various extent. Earlier studies have shown that hydrothermal alteration of the crater-fill suevites (impact melt-bearing breccias) is pervasive in nature and comprises several distinct alteration phases that vary with depth. There is an early phase of K-metasomatism accompanied by minor albitization and chloritization at temperatures of approximately 200–300 ^{o}C [1]. In contrast to the crater-fill suevites the IHT alteration within surficial suevites at the Ries crater is typically restricted to smectite with a composition corresponding to dioctahedral Al-Fe montmorillonite with minor zeolite (mainly phillipsite) deposition within cavities and fractures suggesting formation at weathering conditions [2].

In this paper, we present preliminaryresults of a detailed oxygen and hydrogen stable isotope survey on smectite fraction of crater fill and surficial suevite samples from Ries crarer. The stable isotope study was undertaken in order to eluciate the temperature of the fluids responsible for alteration of impact glass and primary silicate minerals and the formation of secondary clays in Ries crater.

Material and methods: Studied surficial suevite samples that varies from fresh suevite (with no or limited noticeable alteration) to highly altered suevites were collected from 5 outcrops within and around the Ries impact structure, drillcore material were included. The material sampled from the Nördlingen 1973 drill core comprises low- and high-temperature suevites from the suevite sequence 340 m to 525 m interval.

Stable oxygen isotopic composition was measured in clay separates from the suevite matrix at the Stable Isotope Laboratory, University of Lausanne.

Results and discussion: The δ^{18}O values of the smectite in surficial suevites vary between 19 to 23‰ VSMOW. The hydrogen isotope values exhibit rather similar values between the sampled outcrops, with a mean value of –84 ± 2‰, exept one sample R 38 from Aumühle location where the hydrogen isotope value was significantly higher, i.e., -27‰ . Smectite δ^{18}O and δD values in crater-fill suevite samples, however, range from 8‰ to 14‰ and –33‰ to –62‰, respectively.

According to Vennemann et al. [3] the oxygen isotope composition of impact glasses at the Ries crater sampled from widely spaced localities are very homogeneous with δ^{18}O values in the range of 6.7 to 7.4‰. The major modification of the original oxygen values suggests a large water/rock ratio wich suggest significant hydrous alteration and does not support the incipient devitrification mechanism of the impact glass transformation. The siginificant enrichment of the δ^{18}O and δD composition of the monomineral smectite fractions of the surficial suevites suggest low temperature origin of smectite. The crater-fill suevites, however, show a trend of decreasing δ^{18}O values and increasing δD values with increasing depth, from 14‰ and -62‰ at 368 m to 8‰ and -51‰ at 525 m. The different formation temperature of the surficial and crater fill suevites is evident from the estimated fluid temperatures using smectite stable istope geothermometry whichs suggests that the smectite precipitated in equilibrium with meteoric fluid at temperatures ranging from 20 to 25 °C, with exeption of the sample R 38 from the Auhmüle location which suggest ~50 °C. In crater fill suevites the estimated temperatures increase with the depth from 60 °C at 368 m depth to 115 °C at 525 m depth. It is interesting enough that the temperatures of the hydrothermal fluid esitmated from the smectite minerals are 80-180 °C lower that estimated from mineral assocciations earlier (e.g. [1]) suggesting that the smectite formation occured during the latest phase of the impact cooling. Nevertheless, the mineral paragenesis of smectite and zeolite minerals suggest that the smectite was not the last mineral phase forming in Ries hydrothemal systems at it was followed by widespread analcime precipitation probably at temperatures close to ambient.

References: [1] Osinski G. R. (2005) *Geofluids, 5*, 202-220. [2] Muttik N. et al. (2008) *MAPS*, 43, 1827-1840. [3] Vennemann T. W. et al. (2001) *GCA, 65*, 1325-1336.

PRELIMINARY PALEOMAGNETIC STUDY OF ROCKS FROM THE POSSIBLE IMPACT STRUCTURE AT ÅVIKEBUKTEN BAY, NORTHERN SWEDEN. U.Preeden[1], J.Plado[1], V.Puura[1], J.Kirs[1], T.Flodén[2], [1]Department of Geology, University of Tartu, Vanemuise 46, 51014, Estonia (ulla.preeden@ut.ee), [2] Department of Geology and Geochemistry, Stockholm University, S-10691, Sweden.

Introduction: At the time of rock and sediment formation some iron-bearing minerals can record past directions of the Earth's magnetic field. However, this primary magnetic information can be partly or completely destroyed by a secondary magnetic overprint during any geological event after the formation of the rock or sediment. During an impact, processes as the passage of shock waves and associated chemical-mineralogical processes, melting and early post-impact hydrothermal alteration, might de- or remagnetize the target. Under suitable conditions paleomagnetic studies (e.g. Vredefort [1] and Jänisjärvi structure [2]) serve as dating tools for revealing such signatures in the rock's history.

Previous studies: The circular shape of the Åvikebukten Bay, drew attention of the scientists during detailed mapping of the nearby Alnö intrusive complex in the 1960s. The structure was first suggested as an impact structure by H. Henkel and R. Lilljequist [3], based on the extraordinarily circular topography, with a diameter of ~9.5 km at the present erosional level, and the presence of polymict breccia. Later mineralogical and geophysical studies gave further support to impact theory [4]. Mineralogical studies of polymict breccias, found as occasional poorly rounded erratic boulders and cobbles along the rocky beach, revealed number of shock metamorphic features like kink-banding in micas, mosaicism of quartz grains, planar fractures in feldspars and quartz and planar deformation features (PDF). The groundmass of polymict breccia is cemented by carbonatitic (calcitic) masses. In three, out of the 25, studied breccia thin sections planar deformational features (PDF's) in quartz were observed with spacing of about 5 to 8 μm at four crystallographic orientations {1013}, {1012}, {1121} and {2241} [4]. Only one system of PDF's per grain was seen.

Paleomagnetic studies: In order to get hints for origin and approximate age of the structure, and its relation to the nearby carbonatite-alkaline Alnö intrusion complex, in-situ brecciated Precambrian rocks (quartzite) and number of fine- and microclastic breccia veins rich in carbonate cementing mineralization, were sampled for paleomagnetic study at the coastal outcrop along the southern shore of the Bay. Brecciated rocks have previously been described from the outcrop [3], (June, 2008). Altogether 78 cores were drilled: 27 from the quartzite clasts, 26 from the matrix of the brecciated quartzite, and 25 from the fine-grained non-brecciated carbonatitic and microbrecciated carbonate cemented veins cross-cutting the exposure.

Our study shows that quartz clasts from the in-situ brecciated quartzite are non- or weakly magnetic and do not carry stable components. Some breccia matrix samples reveal a few scattered components. The only reliable characteristic low-coercivity remanence component was obtained from the vein material, rich in calcite mineralization similar to Alnö complex rocks. Mean of the component is directed relatively steeply downwards to NE (D = 50.0º; I = 66.3º; k = 194.7, a95 = 8.9º). A paleopole calculated from this direction falls at 59.6ºN, 111.0ºE showing an age of about ~600 Ma (after APWP, [5]). Relatively low coercivity and unblocking temperatures (350…400ºC) indicate pyrrhotite or maghemite as carrier of this remanence.

Conclusion: We find that the obtained remanence direction and its age are very similar to those obtained from the Alnö complex (584 ±7 Ma; [6]) hinting that the Åvike Bay structure is (i) older than Alnö intrusion or (ii) the observed brecciation is related to the formation of Alnö intrusion only. Thus, our results do not support the impact origin for Åvikebukten Bay, however, neither can our data be used to reject it.

References: [1] Salminen et al. (2009) Precambrian Research, 168, 167-184. [2] Salminen et al. (2006) Meteorit. Planet. Sci. 41, 1853–1870. [3] Henkel H. and Lilljequist R. (2001) 6th EFS – IMPACT workshop, Abstract. [4] Henkel H. et al. (2005) in Koeberl, C. and Henkel, H. (eds.), Springer, Berlin, 323-340. [5] Meert J.G. and Torsvik T.H. (2003) Tectonophysics, 375, 261-288. [6] Meert J.G. et al. (2007) Precambrian Research, 154, 159-174.

STRUCTURAL STATE OF SMECTITE AND MIXED LAYER SMECTITE-ILLITE MINERALS AS TEMPERATURE INDICATOR IN IMPACT INDUCED HYDROTHERMAL SYSTEMS: EXAMPLE OF RIES CRATER. P.Somelar, N.Muttik and K.Kirsimäe. Department of Geology, University of Tartu, Vanemuise 46, 51014, Estonia (peeter.somelar@ut.ee).

Introduction: Dioctahedral Al-Fe montmorillonite is the typical secondary mineral forming during the hydrous alteration of the surficial suevites of Ries crater. Muttik et al. (2008) has shown that the composition and structural state of the does not show any significant variation within the structure and forwarded an hypothesis that the fully expandable smectite type minerals in surficial suevites have formed directly by weathering(dissolution) of impact glass to smectite under influence of percolating meteoritic waters.

However, the hydrothermal alteration in crater fill suevites is well defined. Osinski (2005) suggest in Ries argillic alteration (predominantly montmorillonite, saponite, and illite) and zeolitization (predominantly analcite, erionite, and clinoptilolite) with early phase of K-metasomatism accompanied by minor albitization and chloritization at temperatures of approximately 200-300 oC. The source of the fluids for the Ries hydrothermal system were likely a combination of surface (meteoric) waters that percolated down from the overlying crater lake and groundwater that flowed in from the surrounding country rocks into the hydrostatic void created by the impact event (Osinski 2005).

If temperatures in hydrothermal system at Ries reached 200-300 °C, then we could assume the illitization of the smectite type minerals in crater fill suevites.

Material and methods: In this study we investigate the structural state (illitization) of the clay mineral separates of the crater fill suevites in drillcore Nördlingen 1973 of the Ries crater. The structural state of the smectite minerals in crater fill suevites was compared to the smectite minerals in surficial suevites reported in Muttik et al. (2008). The clay fraction (<2 µm) was investigated in oriented preparations using Bruker Discover D8 diffractometer under ambient conditions and after ethylene-glycol (EG) solvation. The measured patterns were analysed using MLM2 and MLM3 codes (Plancon and Drits, 2000).

Results and discussion: Our preliminary results suggest that the smectite type minerals in crater fill suevites are represented by mixed-layer smectite-illite mineral with random ordering (R0). The surficial suevites are without any exception the fully expandable Al-Fe montmorillonite (smectite) minerals. The crater fill material shows, however, up to 20-25% of illitic layers. There is no clear observable tendency of the expandablity changing with the depth of the samples analysed.

The illitization has been shown to be principally controlled by temperature and the onset of the illitization of smectite in bentonites occurs at ~70 °C and the mixed-layer I/S structural ordering transition from R0 to R1 at 35%S at temperatures ~150 °C (Šucha et al., 1993).

This suggests that, at least,during the formation of the smectite type minerals and illitzation the temperatures did not exceeded ~150 °C which should have resulted in significant illitization with the formation of R1 or R2 type mixed-layer illite-smectite minerals.

The estimated temperatures of 70-150 °C are, however, in good accordance with the fluid temperatures estimated from the stable isotope composition of the smectite minerals in crater fill suevites that range from ~60 to ~120 °C (Muttik et al., in this volume).

References:

Muttik, N., Kirsimäe, K., Somelar, P., Osinski, G.R., 2008. Post-impact alteration of surficial suevites in Ries crater, Germany: Hydrothermal modification or weathering processes? Meteoritics and Planetary Science 43. 1827-1840.

Osinski, G.R., 2005. Hydrothermal activity associated with the Ries impact event, Germany. Geofluids 5: 202–220.

Plançon, A., Drits, V.A., 2000. Phase analysis of clays using an expert system and calculation programs for X-ray diffraction by two- and three-component mixedlayer minerals. Clays and Clay Minerals 48, 57–62.

Šucha, V., Kraus, I., Gerthofferova, H., Petes, J., Serekova, M., 1993. Smectite to illite conversion bentonites and shales of the East Slovak Basin. Clay Minerals 28, 243-254.

THE GEOPHYSICAL SIGNATURE OF IMPACT CRATERS

Stephanie Werner, NGU Trondheim, Norway, Stephanie.Werner@ngu.no

Introduction: Unlike most other planetary bodies, the impact crater record on Earth is influenced by geological processes such as erosion and plate tectonics, so that most terrestrial craters are modified or buried (20%) after formation. Though sedimentation protects the crater, it limits the identification based on surface morphology. Therefore, geophysical methods have been proven to be a useful tool in crater recognition. Here, an inventory of methods and signatures is given.

Gravity anomalies result from density variations in the target rocks and reflect a stable bulk rock property. During the crater formation process, brecciation and fracturing occurs, extending to significant depth below the crater floor. The fractured rock is less dense than the unaltered surrounding rock. Additionally, the formation of allochtonous breccia and melt sheets contributes to the gravity signal. Considering that the primary shape of an impact craters is a circular depression, the associated gravity anomaly is usually *negative.* Detailed characteristics depend on size and morphology of the crater, density contrast of shattered and unaltered rock and burial depth. As the complexity of craters grows with diameter, the gravity anomaly amplitude is decreasing, and in extreme cases such as the lunar basins, where the interior is filled with denser volcanic material, the gravity signal inverts and positive gravity anomalies can be observed.

Magnetic anomalies are rather a target property than a direct influence of the cratering process. The anomalies are induced in rocks due to the Earth's magnetic field, and are more complex than gravity anomalies, because of the dipolar character of the magnetic field and the vector properties of the magnetic components (rock and external field). The anomalies reflect variations of magnetic susceptibilities, which need the presence of magnetizable minerals. The anomaly shape itself is depending on the site latitude and polarity of the Earth's magnetic field. Unlike the gravity anomaly there is no specific signature associated with an impact crater, but if existent, it resembles the shape/circularity of the structure. Due to fragmentation and mixing of the target rock, an anomalously low or random magnetic signature can interrupt the regional magnetic pattern. As well as strong local magnetic anomalies can reflect the presence of melt or the uplift and deformation of target material. If the anomaly is related to impact melt, palaeomagnetic dating is possible.

Seismic studies use triggered sound waves, which are reflected or refracted by boundary layers due to property changes (e.g. bulk density) across those boundaries. Seismic methods reveal subsurface deformation, which are distinctive for impact structures, such as modest downward and inward displacement of material along the edges, structural disruption with no coherent seismic reflectors, roughly corresponding to the transient cavity, and the presence of reflectors below the disrupted zone, ruling out other tectonic or volcanic formation processes. These studies are essential for recognizing the structure when the crater is buried under younger sediments or water.

Other methods such as electrical, electro-magnetic or magnetotelluric similarly map rock properties, which can be interpreted as structural information if resulting form impact-related target modification. For example, resistivity variations may indicate an impact-induced, increased porosity and fluid content, resulting in a relative low, which might extend farther than the rim, or due to uplifted (denser) material a relative high.

Summary: Examples for Chicxulub, Vredefort, Roter Kamm, Mjølnir and Gardnos are shown.

The main attribute of the geophysical signature of an impact structure is the resemblance of circularity. Generally, all methods are valuable for crater detection in a geological active environment such as the Earth, though no proof for impact origin is possible through geophysical measurements. Craters show up as negative gravity anomaly. The magnetic signature is target dependent (presence of magnetic mineral assemblages) and commonly more complex than the gravity anomaly. Detailed structural information can be gathered by seismic studies. Potential field modelling of the subsurface structure is more successful when calibrated with target properties collected from drill cores, and supported by seismic information.

References: Pilkington & Grieve (1992) Reviews of Geophysics 30,2, 161-181. Henkel (1992) Tectonophysics, 216,1/2,63-90.

FORMATION AND EMPLACEMENT OF IMPACTITES IN LARGE TERRESTRIAL IMPACT STRUCTURES. Axel Wittmann, Lunar and Planetary Institute, 3600 Bay Area Boulevard, Houston, TX. 77058, wittmann@lpi.usra.edu.

I. Introduction

Formation and emplacement conditions of impactites are recorded in their petrologic inventory. This information can be unraveled by systematic petrographic analyses. Such data is useful for the reconstruction of impact cratering events, which are fundamental geological processes on the terrestrial planets. It is therefore arguable that the determination of physical boundary conditions of impact events is a prerequisite for understanding Earth's planetological context.

II. Phenomenology

In the first phase of the impact cratering process, compression from the propagating shock wave and the subsequent release from these shock pressures produces characteristic deformation features in target rocks. A hemispheric melt zone develops that engulfs the region in the target that was subjected to shock pressures ~60-100 GPa. In this pressure regime, whole rock melts are produced from quartzo-feldspathic upper crustal rocks [1]. In large terrestrial impacts, gross homogenization of impact melt is typically attained due to the high turbulence and the energetic nature of the crater forming process. At the same time the shock pressures are being released, an ejecta plume develops, which consists of a highly dynamic mixture of vaporized and melted target rock, projectile material, and solid rock debris [2]. It forms from extreme starting conditions with pressures of several 100 GPa and temperatures of >10,000 °C and expands in its early phase with a velocity of >5 km/s, decelerates, and collapses [3,4]. Products of this collapse are suevite rocks [5].

III. Methods

The formation and emplacement of impactites has been studied in the ~180 known impact structures on Earth, using theoretical models, analog materials, and spacecraft data from the terrestrial planets. Recognition of impact structures on Earth requires the identification of macroscopic (mostly structural geologic) and microscopic (mostly petrographic and geochemical) characteristics. Because endogenic processes rapidly modify ejecta deposits, sufficiently abundant and continuous impactites are found in the topographic depression within the trace of the transient cavity. Drill cores and outcrops of such crater-fill sequences provide sample materials for study.

IV. Case studies

Drill core samples and photographic documentation of impact melt-bearing crater-fill deposits from the Yaxcopoil-1 drill core (Chicxulub) and the Eyreville-B drill core (Chesapeake Bay) were used to reconstruct cratering processes. Petrographic information was extracted from thin sections and drill core photographs were studied by image analytical techniques.

Chicxulub: The 1551 m deep Yaxcopoil-1 corehole is located ~45 km from the center of the ~180 km diameter, 65 Ma old Chicxulub impact structure [6]. Structurally, it is located in the annular moat, just outside the limits of the transient cavity. The basal ~515 m are mainly composed of carbonate and evaporite sedimentary rocks. Based on structural characteristics and the occurrence of rare polymict impact breccia dikes, this section is interpreted as displaced megablocks that were exclusively derived from the ~3-5 km thick sedimentary cover rocks of the target [7]. These megablocks are overlain by a 100 m thick section of suevites and brecciated impact melt rocks. Based on petrographic characteristics, this section can further be subdivided into a basal portion of suevites that contain abundant carbonate target material. Melt particles in these suevites do not exhibit shapes that are interpreted to indicate airborne transport. Instead, turbulent fragmentation and elongation of melt particles suggest ground-surge deposits [6, 8]. These are capped by ~24 m of brecciated impact melt rocks that contain little clastic debris. Hyaloclastite-like fragmentation of these melt rocks is indicative of explosive fragmentation due to the release of volatiles. This melt rock unit is overlain by a complex suevitic ejecta-plume deposit: Immediately above the brecciated melt rock, suevites indicate the erosive collapse of a hot protion of the ejecta plume which produced thermal softening of melt fragments [8]. This is followed by a gradual reduction of turbulence and temperatures, and the mixing-in of different melt particle types. The uppermost 26 m of suevites exhibit increasing degrees of component size-sorting and rapid quenching features. This is interpreted as a graded fall-back deposit that likely recorded the late-stage collapse of the ejecta plume until ~10 minutes after the cessation of turbulent conditions above the crater [6]. Minor aquatic reworking is indicated in a ~60 cm thick section on the very top of the suevites, suggesting that this region of

the crater was not affected by immediate oceanic resurge. More likely, gradual infilling by the Tertiary ocean resulted in the deposition of ~800 m of carbonates and evaporites at Yaxcopoil-1.

Chesapeake Bay: The ICDP-USGS Eyreville boreholes through the annular moat of the 85 km diameter Chesapeake Bay impact structure were drilled ~9 km NNE' from its center. These drill cores recovered a continuous 154 m section of polymict impact breccias [9]. These rocks record cratering processes before burial with ~1 km thick resurge deposits. A plausible petrogenetic scenario invokes a lower block-rich section that slumped from an outer region of the transient cavity into the annular moat towards the end of crater excavation. This blocky debris was mixed with remains of the excavation flow. Subsequently, melt-rich suevites were emplaced that recorded interaction of the expanding ejecta plume with fallback material related to the evolving central uplift [10]. Clast-rich impact melt rock that likely shed off the central uplift covers these suevites. Incipient collapse of the ejecta plume is recorded in the uppermost, ~ 5 m thick subunit, but the arrival of oceanic resurge flow into the crater terminated its continuous deposition ~6-8 minutes after impact [11]. The duration of fallback from the ejecta plume is recorded by a melt-shard horizon in the resurge deposits. A mere ~15 m below the transition to background sediments, this shard horizon formed from late fallback from the ejecta plume into the resurge flow within 15 minutes after the initial impact [12]. This also constrains deposition of ~1 km of resurge debris within ~10 minutes. Nonetheless, lack of hyaloclastic fragmentation of impact melt rocks suggests their emplacement under dry conditions [13]. The low estimated quantity of impact melt in the crater (~10 km^3) remains elusive. Possible causes may relate to increased excavation efficiency due to 1) a high ratio of water column and sedimentary target to depth of excavation, 2) an oblique impact, or 3) a buried melt sheet at depth.

V. Outlook

The petrogenetic scenarios for the Chicxulub and Chesapeake Bay impactites are based on unidimensional petrographic information. The two case studies will have to be tested with further sampling campaigns. Because terrestrial impact structures form in widely differing geological settings, comprehensive studies are required to reconstruct specific cratering events. With that regard, the study of impact craters with preserved ejecta deposits offers the opportunity to unravel emplacement processes and test various current models for their formation. A refined understanding of terrestrial impactites will be crucial for the future exploration of the terrestrial planets.

Acknowledgments:

I thank Henning Dypvik and the organizers of the Network on Impact Research Workshop for the invitation to participate. These studies were made possible by the contributions and support from Dieter Stöffler, Thomas Kenkmann, Ralf-Thomas Schmitt, Lutz Hecht, Uwe Reimold, Peter Czaja and Hans Rudolf Knöfler (Museum für Naturkunde Berlin), David Kring (LPI Houston), Wright Horton Jr. (USGS Reston), and Sonia Boyum.

References:

[1] Stöffler, D. & Grieve, R. A. F. (2007) Impactites, Chapter 2.11 In *Metamorphic Rocks: A Classification and Glossary of Terms, Recommendations of the International Union of Geological Sciences Subcommission on the Systematics of Metamorphic Rocks* (D. Fettes & J. Desmons), pp. 82-92, 111-125, 126-242, Cambridge University Press. [2] Pierazzo E. et al. (1998) Hydrocode simulation of the Chicxulub impact event and the production of climatically active gases. *J. Geophys. Res.* **103**(28), 28607-28626. [3] Melosh H. J. (1991) Atmospheric impact processes. *Adv. Space Res.* **11**(6), (6)87 - (6)93. [4] Shuvalov V. (2003) Displacement of target material during impact cratering. In *Impact markers in the stratigraphic record* (eds. C. Koeberl and F. Martínez-Ruiz), pp. 121-135. Springer. [5] Kieffer S. W. & Simonds C. H. (1980) The role of volatiles and lithology in the impact cratering process. *Rev. Geophys. Space Phys.* **18**, 143-181. [6] Stöffler D. et al. (2004) Origin and emplacement of the impact formations at Chicxulub, Mexico, as revealed by the ICDP deep drilling Yaxcopoil-1 and by numerical modeling. *Met. Planet. Sci.* **39**, 1035-1068. [7] Kenkmann T.et al. (2004) Structure and impact indicators of the Cretaceous sequence of the ICDP drill core Yaxcopoil-1, Chicxulub impact crater, Mexico. *Met. Planet. Sci.* **39**, 1069-1088. [8] Wittmann A. et al. (2007) Reconstruction of the Chicxulub ejecta plume from its deposits in drill core Yaxcopoil-1. *GSA Bull.* **119**, 1151-1167. [9] Gohn G. S. et al. (2008) Deep Drilling into the Chesapeake Bay Impact Structure. *Science* **320**, 1740-1745. [10] Wittmann A. et al. (2009) The record of ground zero in the Chesapeake Bay impact crater - suevites and related rocks. In *GSA Spec. Pap. 458*. [11] Collins G. S. & Wünnemann K. (2005) How big was the Chesapeake Bay impact? Insight from numerical modeling. *Geology* **33**(12), 925-928. [12] Kenkmann T. et al. (2009) A model for the formation of the Chesapeake Bay impact crater as revealed by drilling and numerical simulation. In *GSA Spec. Pap. 458*. [13] Wittmann A. et al. (2009) Petrology of impact melt rocks from the Chesapeake Bay crater, USA. In *GSA Spec. Pap. 458*.

SCALING OF CRATER FORMATION - NUMERICAL MODELLING OF IMPACT PROCESSES ON CONTINENTAL TARGETS K. Wünnemann, Museum für Naturkunde - Leibniz-Institute at Humboldt University Berlin, Invalidenstrasse 43, 10115 Berlin, Germany (Contact: kai.wuennemann@mfn-berlin.de).

Introduction: The dimensions of meteorite impact craters provide an important measure of the energy that was released by an impact event. To evaluate the consequences accompanying the strike of a meteorite, therefore, it is of particular importance to find a relationship between crater size and impact energy. Deducing the original size of the impactor from a given crater size is impossible because velocity, impact angle and material properties are usually unknown. The inverse question, however, of how large a crater will be produced by an impact of given size, mass, velocity, and angle of incidence has been investigated in many experimental [1,2] and numerical modeling studies [3], which have resulted in the development of so-called scaling laws.

A fundamental assumption underlying cratering scaling laws is that an impact event may be approximated as a stationary point source of energy and momentum buried at a certain depth in the target, analogous to the detonation center of an explosive source [4,5,6,7]. If this assumption holds true for any hypervelocity impact, the kinetic energy (and momentum) of the impactor that is effectively available as an energy (and momentum) point source is defined, according to the theory, by the so-called coupling parameter. It is assumed that the coupling parameter combines the properties of the impactor (velocity U, diameter L, density δ) into one scalar parameter: $C=LU^{\mu}\delta^{\nu}$ [6]. In two theoretical end-member cases, the coupling parameter is exactly proportional to the kinetic energy (where ν=1/3, μ=2/3) or the momentum (ν=1/3, μ=1/3) of the impactor, respectively. However, experimental evidence suggests that the coupling parameter is somewhere between these limits; in other words, it is proportional to some combination of kinetic energy and momentum (ν=1/3; 1/3<μ<2/3) [6]. The exact form of the coupling parameter appears to depend on target properties. In addition, impact angle plays an important role [8] and has not yet been successfully incorporated into scaling laws.

Pi-group scaling: The primary purpose of scaling laws is to meaningfully extrapolate the results of small scale laboratory impact experiments so that they may be applied to large scale natural craters. To achieve this, dimensionless ratios are used to estimate the relative importance of different physical processes during crater formation. Dimensionless measures of the properties of impactor and target can be related to scaled crater dimensions implying that the relative crater size is independent of the real size of an impact event.

The most successful approach in dimensional analysis of impact crater scaling is the so-called Pi-group scaling [4]. Instead of defining for instance the crater volume V as function of six (or more) target and projectile properties (e.g., V=F(U,ρ,δ,Y,g,m), where U is impact velocity ρ is target density, δ is projectile density, Y is strength, g is gravity, and m is projectile mass) the use of dimensionless ratios reduces the number of independent variables to three: π_V=F(π_2,π_3,π_4), where the so-called crater efficiency $\pi_V = \rho V/m$, the gravity-scaled size of an impact event π_2=1.61gL/U^2, and the strength-scaled size $\pi_3= Y/(\delta U^2)$, and the density ratio $\pi_4=\rho/\delta$. Note that the angle of impact θ is yet not considered in this concept (compare [9]).

The assumption that an impact can be represented as a stationary point-source has been shown to imply that many impact-related phenomena are related to the dimensionless ratios π_2, π_3 and π_4 by power laws. For instance, if gravity is the dominant influence on crater growth, crater efficiency π_V can be expressed as a power-law of π_2 and π_4: $\pi_V=C_V\,\pi_4^{\alpha}\,\pi_2^{\beta}$, where the exponents α, β are related to the exponent in the coupling parameter: β=-3μ/(2+ μ), and α=(2+ μ -6ν)/(2+ μ) [4]. A large number of impact experiments in sand and water and numerical modeling of crater formation have demonstrated the utility of this, and other power law relationships, over a large parameter range.

The effect of impact angle on crater dimensions and morphology: Although nearly all impacts occur at an oblique angle of incidence the vast majority of impact structures that can be observed on planetary surfaces are more or less circular in shape. It is well known that the angle of impact affects crater efficiency [2] the propagation of shock waves, and the generation and distribution of impact melt [10], and may also influence the expansion of the ejecta plume. Crater shape, however, seems to be unaffected by the angle of impact. This may be unintuitive, but is conform with the assumption that an impact can be considered as a point-source (see previous section) analogous to an explosion. Nevertheless, detailed morphological and morphometric data from field studies and remote sensing revealed that minor deviations exist [e.g. 11, 12, 13, 14, 15, 16, 17]. Whether these asymmetries result from oblique impacts or are due to pre-impact existing target heterogeneities can be investigated by numerical modeling. Figure 1 shows is series of snapshots of different stages of crater formation for oblique impacts. Apparently, the central part of the crater (central uplift) shows most asymmetries (apart from the distribution of ejecta).

Additionally, numerical model allow for quantifying the effect of impact angle on crater size. Figure 2 shows the considerable reduction in crater efficiency as a function of impact angle. The data for oblique impacts can still be approximated by a power-law if the velocity U is replaced by the vertical velocity component u_v=sinθ U in the definition

of the gravity-scaled sized of an event π_2: $\pi_V = C_V \pi_4^{\alpha} \pi_2^{\beta} \sin^{-2\beta} \theta$ [8,9].

Conclusion: To investigate crater dimensions and crater morphology as a function of projectile properties (impact velocity, size, density, angle of incidence) and target characteristics (density, coefficient of friction, cohesion, porosity, gravity) numerical modeling is an important tool supplementing experimental studies. Moreover, computer simulations of impact processes enable to study crater formation at all stages and allow for investigating the effect of scale-dependent parameters such as gravity on crater dimensions. In particular numerical models provide important insight on the effect of the angle of incidence on crater size and crater morphology under the influence of gravity.

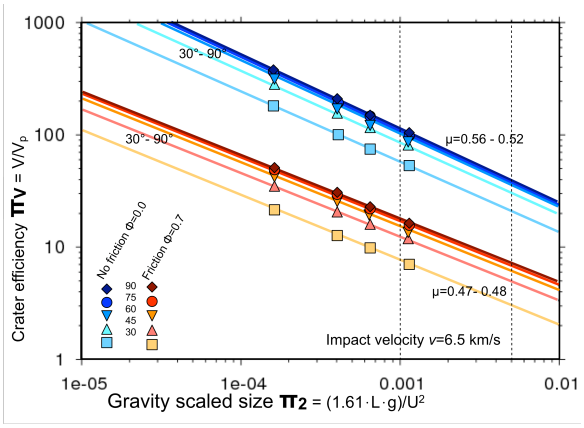

Fig. 2: Gravity-scaled size π_2 versus crater efficiency π_V for oblique impacts (θ=30°-90°) and different friction coefficients ϕ. Blue lines correspond to a ϕ =0.0, yellow-red lines correspond to ϕ=0.7. The impact velocity was 6.5 km/s in all models.

References: [1] Schmidt, R. M. and Housen, K. R. (1987) IJIE, 5, 543-560; [2] Gault, D. E., Sonett (1982), GSA Special Paper 190, 69-92; [3] O'Keefe J.D., Ahrens T.J. (1993), JGR, 17,011-17,028; [4] Holsapple K.A., Schmidt R.M. (1987) JGR, 6350-6376; [5] Holsapple K.A. (1987), Int. J. Impact. Engng., 343-355; [6] Holsapple K.A. (1993), Annu. Rev. Planet. Sci. 12:333-73; [7] Housen K.R., Holsapple K.A. (2003), Icarus, 102-119; [8] Elbeshausen D., Wünnemann K., Collins G.S. (2008), LPSC XXXIX, 1795; [9] Chapman, C. R. and McKinnon, W. B. (1986), Satellites, Univ. of Arizona Press, 492-580; [10] Pierazzo E., Melosh H. J. (2000). Icarus 145, 252-261; [11] Wallis D. et al. (2005). Mon. Not. R. Astron. Soc. 359, 1137-1149. [12] Schultz P. H., Anderson J. L. B. (1996). Geol. Soc. Am. Spec. Paper 203, 397-417. [13] Poelchau M. H. et al. (2007). LPS XXXVIII, Abstract #1698. [14] Scherler D. et al. (2006). EPSL 248, 28-38. [15] Herrick R. R., Forsberg-Taylor N. K. (2003). Meteor. Planet. Sci. 38 (11) 1551-1578. [16] Shuvalov V.V. (2003). LMI III, Abstract #4130. [17] Ekholm A. G., Melosh H. J. (2001). Geophys. Res. Letters 28 (4), 623-626.

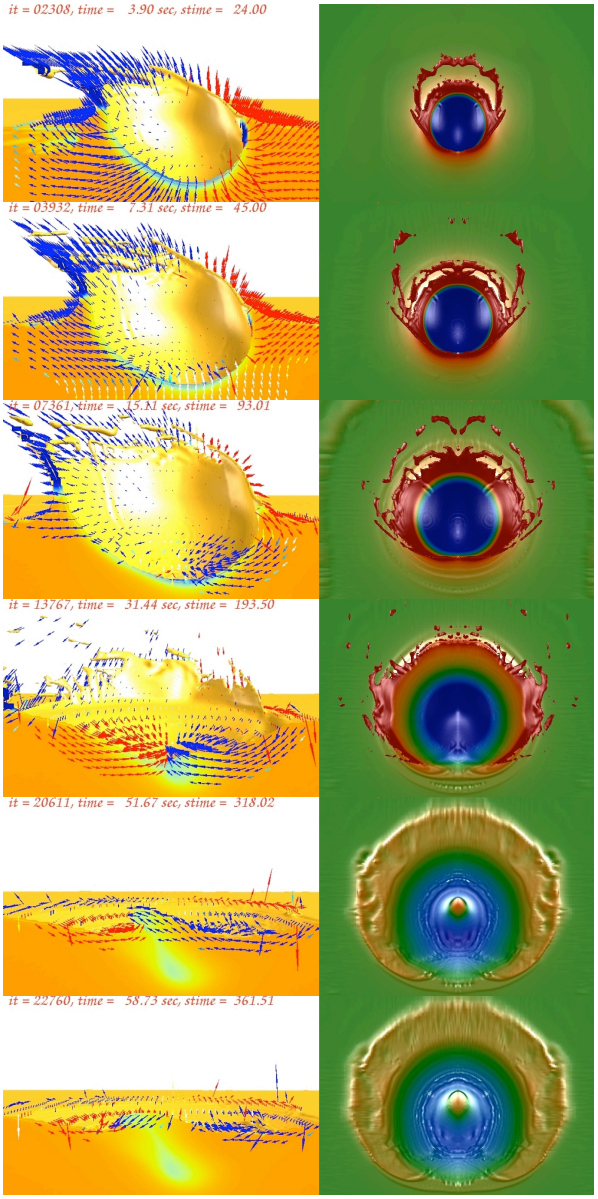

Fig. 1 Snapshots of central peak formation. Impact of a 1km-sized granitic projectile with an impact velocity of 6.5km/s. Impact angle is 30°. Left column: Cross section through the symmetry plane depicts material density, material flux is indicated by arrows which are scaled with absolute velocity and colored by the radial velocity component (blue: flux downrange, red: flux uprange). Impact direction is from right to left. Right column: Plane view of the crater. Topography is colored by height. Impact direction from bottom to top.

FOUR HUNDRED YEARS OF HITS AND MISSES IN SCIENTIFIC IMPACT CRATER RESEARCH.

T. Öhman[1,2]. [1]Division of Geology, Department of Geosciences, and [2]Division of Astronomy, Department of Physical Sciences, P.O. Box 3000, FI-90014 University of Oulu, Finland, (teemu.ohman@oulu.fi).

Introduction: The year 2009 is the International Year of Astronomy, celebrating the first astronomical use of telescope by Galileo Galilei (1564–1642) and the publication of Johannes Kepler's (1571–1630) first two laws of planetary motion. This year should also be the 400th anniversary of scientific impact crater research, as Galilei was the first modern scientist to describe impact craters. However, progress in impact research after Galilei's first descriptions on lunar craters was very slow, and many perceptions currently regarded as erroneous persisted for centuries. Nevertheless, some fairly early ideas were also surprisingly modern.

Galilei, Hooke, and other giants: Scientific impact crater research began in Padua, Italy, in late November 1609. Galilei's lunar observations, which he published the following year, were very crude in modern standards, due to the limited field of view and optical quality of his telescopes. Thus, his sketches cannot be reliably correlated with specific craters. What Galilei saw was that the lunar surface – assumed previously to be perfectly smooth – is filled with depressions that have uplifted rims. Unfortunately he didn't draw central peaks, but his written descriptions indicate that he actually saw them. Although Galilei compared the lunar "large spots" to terrestrial oceans, it was Kepler who presumed – like Plutarch in the first century A.D. – that they were filled with water. Thus, he coined the term *maria* for them, still used today.

By the time of Robert Hooke (1635–1703) the telescopes had developed greatly, and Hooke published a very good sketch of the crater Hipparchus in 1665. Importantly, he was the first experimentalist in crater research. He dropped bullets to a mixture of pipe clay and water, but although the produced craters resembled the lunar ones, he was forced to abandon the impact hypothesis because he couldn't accept the idea of soft lunar surface, and particularly because his cosmos was void of falling bodies. Instead, he opted for the internal origin of craters, similar to the ones he observed in an experiment involving a pot of boiling alabaster. Another Hooke's mistake was that he thought vegetation grew on the lunar surface.

Edmond Halley (1656–1742) was a versatile researcher, mostly known for his comet studies. However, he also suggested that cometary impacts might cause world-wide catastrophes, and that the Caspian Sea was an impact structure. He had calculated that the biblical flood could not have been caused by 40 days of rain, so he suggested that a massive impact had tilted Earth's axis, causing the flood due to oceans changing their locations. He also promoted the idea that stones allegedly fallen from the sky – meteorites – actually originated from space. Other prominent scientists who believed impacts could have catastrophic consequences were Pierre-Louis Moreau de Maupertuis (1698–1759) in 1750 and Pierre Simon de Laplace (1749–1827) in 1797.

Slow progress: Johann Hieronymus Schröter (1745–1816) was apparently the first to use the term "crater" with respect to Moon in 1791, further emphasizing the assumed volcanic nature of these structures. However, in the 19th century the space was no longer empty, as the first asteroids were discovered and meteorites were generally accepted to have an extraterrestrial origin. Thus, impact theories were proposed by various researchers, but no significant new ideas emerged. Lunar craters firmly remained volcanic – volcanism was, after all, a proven method to produce craters. The absurdity of many of the impact theories didn't help either. For example, as a result of his powdery experiments, Albrecht Meydenbauer proposed in 1877 and 1882 that craters originate as cosmic balls of dust slowly hit the equally dusty Moon. The maria, however, were created when originally Earth-orbiting bodies of sulphur or phosphorus impacted the Moon.

The most famous impact "lunatic" was Franz von Paula Gruithuisen (1774–1852), whose ideas of onion-structured projectiles hitting the plastic surface of the Moon and Earth gained some popularity. He since achieved notoriety by "observing" fields, cows and "lunites", who worshipped stars in their star-shaped temple. A similar impact model was proposed as late as 1909 by the equally notorious Thomas Jefferson Jackson See (1866–1962). This lack of progress in early days of impact studies is no surprise, given that even in 1926 several English researchers believed the lunar craters were glaciers.

Among the more sensible impact theories of the late 19th century were those by August and Heinrich Thiersch. They suggested in 1879 and 1883 that not only the smaller lunar craters, but also Mare Imbrium was the result of a great impact. The most advanced ideas, however, came from Richard Anthony Proctor (1837–1888). In his works from 1877 onwards he proposed that the lunar craters were traces of ancient bombardment that had accreted the Moon. The surface of the Earth lacked craters only because they were demolished by active geologic processes. Among Proctor's mistakes was his presumption that the Moon had been plastic when the impacts occurred. That allowed him to explain the craters' consistently puzzling circularity.

Proctor was close to the solution: he correctly proposed that the projectiles were vaporized upon impact. This was suggested by several other authors too, but it wasn't until the independent works of Ernst Julius Öpik (1893–1985), Herbert Eugene Ives (1882–1953), and Algernon Charles Gifford (1861–1948) in 1916, 1919, and 1924, respectively, that clearly established the importance of explosion in the formation of impact craters. However, none of these studies made any impact at the time, and the vast majority of the very few lunar researchers maintained the volcanic model.

G. K. Gilbert – authority and dilettante: Grove Karl Gilbert (1843–1918) was the chief geologist of the USGS, and therefore a respected figure in geology. In 1891 Gilbert got interested in Coon Mountain, later known as Meteor Crater. He did field studies in the crater, including what apparently was the world's first magnetic survey of an impact crater. As he didn't find a large meteoritic iron mass, he concluded that the crater was produced by a volcanic steam explosion. Thus, the abundance of Canyon Diablo iron meteorites around the crater was merely coincidental.

Gilbert didn't limit his crater studies to the Meteor Crater. He carried out various impact experiments: in addition to more sophisticated high-velocity studies, he was also dropping marbles to porridge. Highly unusually for an eminent geologist of the time, he observed lunar craters too. He showed that 45° is the most probable impact angle, and was the first to note the "Imbrium sculpture", a clear indication for the idea that Mare Imbrium had an impact origin. In addition, he understood its possibilities for relative dating of the lunar surface.

Similar to the Thierschs' idea, he assumed the Earth once had a ring like Saturn, the particles of which subsequently formed the Moon. To avoid the problem of the absent elliptical craters, in his model the last ring particles hit relatively straight the lunar surface. This was necessary because although he emphasized that impacts create a lot of heat – even enough to melt silicates – he didn't understand the explosive nature of the release of that heat.

It is one of the great ironies in the history of science that in a field where Gilbert was an authority, he was utterly wrong, whereas in a field where he was regarded as a dilettante and thus was totally ignored, he was correct in many ways. Therefore, regardless of all the pioneering work he did, he didn't have a general positive effect in neither terrestrial nor lunar crater studies.

Terrestrial craters: The futile attempts of lawyer, mining engineer and entrepreneur Daniel Moreau Barringer (1860–1929) and his early associate Benjamin Chew Tilghman to find a mass of nickel-iron beneath the floor of Meteor Crater – and fight the quiet Gilbert – in early 1900's are well-known. What they did manage to accomplish, however, was that more and more scientists began to accept the idea that the Meteor Crater was of impact origin. One of these scientists was the great Alfred Lothar Wegener (1880–1930). In addition to compiling an excellent review on theories of lunar crater formation, he conducted impact experiments and visited Kaalijärv crater field in Estonia in 1927. He was convinced of its impact origin, but the proof in the form of meteoritic iron was found by Ivan A. Reinvald (1878–1941) a decade later. Thus, the Meteor Crater was no longer unique. And perhaps older impact structures could be discovered too.

John Daniel Boon, Sr. (1874–1952) and Claude Carroll Albritton, Jr. (1913–1988) published a series of insightful papers in late 1930's, unfortunately all in an obscure journal. In addition to correctly proposing an impact origin for several "cryptovolcanic" structures like Flynn Creek, Sierra Madera and Vredefort, as well as for the lunar craters, they presented astoundingly modern ideas in some aspects of cratering mechanics. They suggested that the stratigraphic uplift in craters' central peaks is about 0.1×D, i.e. similar to the currently accepted approximation. They also proposed that the obliquity of an impact might be deduced from structures in the rocks even if the actual crater has been practically eroded away. In this respect they were 70 years ahead of their time.

Conclusions: The first 300 years of impact crater research were the time of very slow progress. Hypotheses of impacts were published by the most prominent scientists, but volcanism had the benefit of being a common, reasonably well-understood process that evidently produced craters all the time. Thus, even the correct and well-presented ideas had no influence on the general scientific thinking. It wasn't until 1940's and the great works of Ralph Belknap Baldwin (1912–) and Robert Sinclair Dietz (1914–1995) that impact cratering started to gain more support. However, the birth of modern impact science had to wait until the Cold War space race and Eugene Merle Shoemaker (1928–1997). And even today, despite claims to the opposite, impact crater research is far from mainstream science.

Acknowledgements: The Network on Impact Research and the efforts of H. Dypvik and E. Kalleson on running it are gratefully acknowledged. **References:** This abstract has drawn from a large number of references, some of the most recommendable being: [1] Galilei G. (1610/1999). *Sidereus Nuncius.* Ursa, 296 p. [2] Hooke R. (1665). *Micrographia.* E-book, www.gutenberg.net. [3] Gilbert G. K. (1893). *Phil. Soc. Washington Bull. 12,* 241–292. [4] Gilbert G. K. (1896) *Science 3,* 1–13. [5] Wegener A. (1921/1975). *The Moon 14,* 211–236. [6] Boon J. D. and Albritton C. C. (1937) *Field and Laboratory 5,* 53–64. [7] Hoyt W. (1987). *Coon Mountain Controversies.* Univ. of Arizona Press, 442 p. [8] Mark K. (1987). *Meteorite Craters.* Univ. of Arizona Press, 288 p. [9] Papers in *Earth Sciences History 17* (1998), 77–209.

E-mail addresses

Katerina Bartosova katerina.bartosova@univie.ac.at , University of Vienna.

Henning Dypvik henning.dypvik@geo.uio.no , University of Oslo.

Galen Gisler galen.gisler@fys.uio.no , University of Oslo.

Steven Goderis Steven.Goderis@vub.ac.be, Vrije University, Brussel.

Sanna Holm Sanna.Holm@geol.lu.se Lund University.

Andreas Jahn Andreas.Jahn@mfn-berlin.de , Humboldt University Berlin.

Tom Øivind Jahren tom.jahren@ramboll.no , Rambøll Norge.

Elin Kalleson elinkal@geo.uio.no , University of Oslo.

Afsoon Moatari Kazerouni afsoon.moatari@geo.au.dk , Aarhus University.

Thomas Kenkmann Thomas.Kenkmann@mfn-berlin.de , Humboldt University Berlin.

Tomas Kohout tomas.kohout@helsinki.fi , University of Helsinki.

Svein Olav Krøgli sveinkro@geo.uio.no , University of Oslo.

Nele Muttik nele.muttik@ut.ee, University of Tartu.

Ulla Preeden ulla.preeden@ut.ee University of Tartu.

Peter Somelar psomelar@ut.ee , University of Tartu.

Teemu Öhman teemu.ohman@oulu.fi University of Oulu.

Stephanie Cristine Werner Stephanie.Werner@NGU.NO , Norwegian Geological Investigation, Trondhjem.

Axel Wittmann Wittmann@lpi.usra.edu , Lunar and Planetary Institute, Houston.

Kai Wünnemann kai.wuennemann@mfn-berlin.de , Humboldt University Berlin.